

Local and global controls on carbon isotope chemostratigraphy

Anne-Sofie C. Ahm^{*1, 2} and Jon M. Husson²

¹*Princeton University, Guyot Hall, Princeton, NJ 08540, USA*

²*University of Victoria, School of Earth and Ocean Sciences, BCV8W 2Y2 Canada*

March 10, 2021

This is a non-peer reviewed preprint submitted to EarthArXiv. The manuscript is currently in review for publication in Cambridge Elements. Please note that following peer-review, subsequent versions of this paper may have slightly different content.

^{*}Corresponding author: aahm@princeton.edu

Abstract: Over million-year timescales, the geologic cycling of carbon controls long-term climate and the oxidation of Earth’s surface. Inferences about the carbon cycle can be made from time series of carbon isotopic ratios measured from sedimentary rocks. The foundational assumption for carbon isotope chemostratigraphy is that carbon isotope values reflect dissolved inorganic carbon in a well-mixed ocean in equilibrium with the atmosphere. However, when applied to shallow-water platform environments, where most ancient carbonates preserved in the geological record formed, recent research has documented the importance of considering both local variability in surface water chemistry and diagenesis. These findings demonstrate that carbon isotope chemostratigraphy of platform carbonate rarely represent the average carbonate sink or records changes in the composition of global seawater. Understanding what causes local variability in shallow-water settings, and what this variability might reveal about global boundary conditions, are vital questions for the next generation of carbon isotope chemostratigraphers.

1 Introduction

2 The geologic carbon cycle is central to our understanding of the evolving habitability of planet
3 Earth. The solid Earth outgasses carbon as CO₂ to the ocean-atmosphere system, and sedimentary basins bury carbon as either carbonate minerals (calcite, CaCO₃, or dolomite, CaMg(CO₃)₂)
4 or organic matter (CH₂O). The burial of carbonate is a product of chemical weathering of igneous minerals, which generates the necessary alkalinity for carbonate mineral precipitation from
5 seawater. Owing to a temperature-dependence of chemical reaction rates, chemical weathering
6 (and associated carbonate burial) acts as a planetary thermostat, regulating the greenhouse gas
7 CO₂ and stabilizing global temperatures on long timescales (>10⁵ years, Walker et al. 1981). By
8 contrast, organic matter formation is the result of biological activity. If the product of oxygenic
9 photosynthesis, CO₂ + H₂O ⇌ CH₂O + O₂, the burial of organic carbon results in the net
10 release of free O₂ to the surface environment.

13 Sedimentary burial fluxes of carbon are connected both to the long-term maintenance of an
14 equitable climate (e.g., Walker et al. 1981) and the oxygenation of the surface of Earth (Broecker
15 1970). However, direct constraints on carbon burial fluxes, and their use to study Earth history,
16 are rare, owing both to the difficulties in building geologic syntheses of sedimentary volumes
17 (Ronov et al. 1980) and to the uncertainties surrounding how erosion and rock cycling have
18 affected such records (Gregor 1970). As a result, the measurement of proxies is the dominant
19 approach for the study of the ancient carbon cycle – specifically, the measurement of the ratio of
20 stable carbon isotopes (¹²C and ¹³C) in carbonate rocks and sedimentary organic matter. Under specific assumptions about both how carbon behaves in the ocean-atmosphere system and
21 how surface geochemistry is recorded in the sedimentary record, inferences about the geologic
22 carbon cycle can be made from time series of carbon isotope ratios. These inferences include
23 the origin of life (Schidlowski et al. 1975), transient increases in atmospheric CO₂ (e.g., Berner
24 2006) and the burial history of organic carbon across the Phanerozoic (Broecker 1970) and Pre-
25 cambrian (Knoll et al. 1986). By direct consequence of this interpretative framework, carbon
26 isotopic values can be used as tools of stratigraphic correlation. Namely, on timescales of sedi-
27 mentary rock formation, perturbations and changes to the carbon cycle should be recorded in
28 globally-disparate basins as synchronous events, and thus useful as chronostratigraphic markers
29 for intra-basinal and inter-basinal correlation models. This application is referred to as *carbon*
30 *isotope chemostratigraphy*, and is relied upon heavily for the study of the Precambrian, when
31 index fossils needed for biostratigraphy are lacking (Knoll et al. 1986).

34 In this review, we highlight the developments, potential pitfalls, and future potentials of carbon
35 isotope chemostratigraphy. As we explain below, the validity of its application is dependent on
36 assumptions about the global carbon cycle, and about how the isotope geochemistry of sedimen-
37 tary carbonates and organic matter records conditions of the surface environment from which

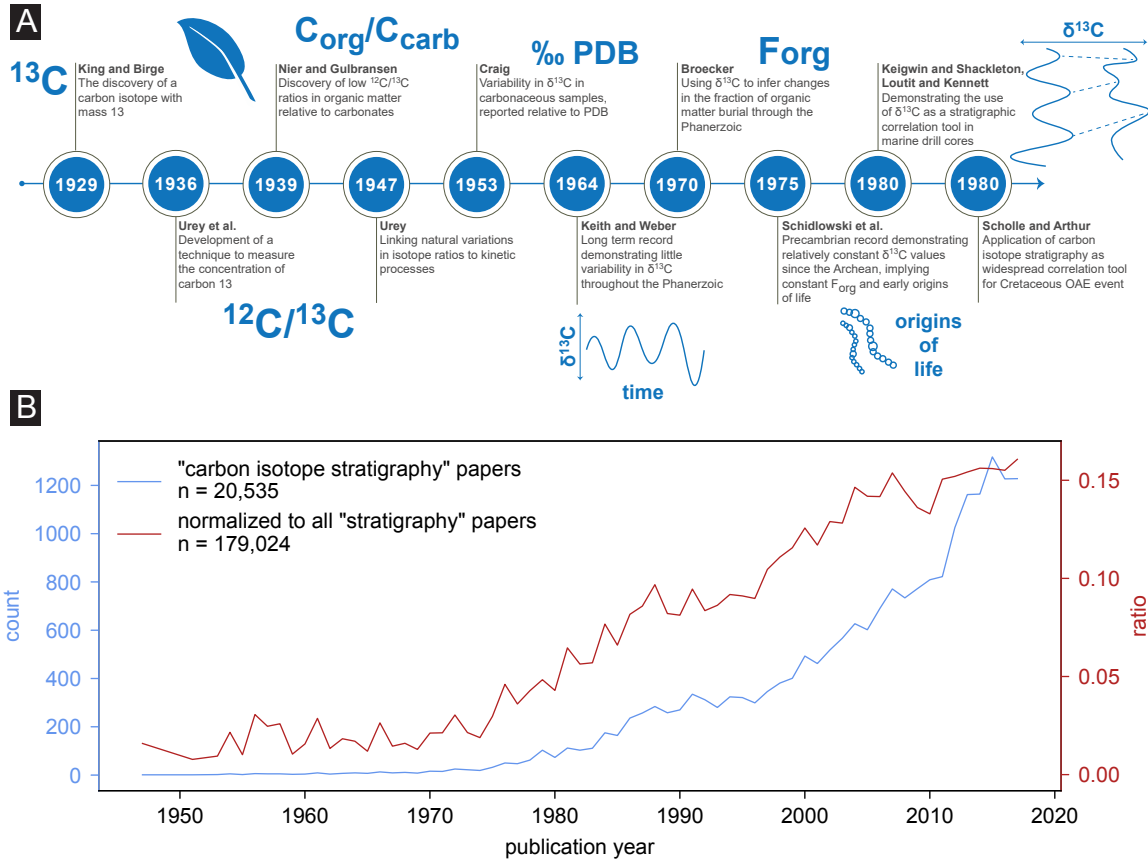


Figure 1: (A) The early history of carbon isotope research, from the discovery of ^{13}C in 1929 (King and Birge 1929) to 1980, listing some of the most consequential papers that underpin the development of carbon isotope chemostratigraphy. (B) The number of peer-reviewed papers published per year that contain the phrases ‘carbon isotopes’ and ‘stratigraphy’ (blue, left y-axis), extracted from the GeoDeepDive digital library (<https://geodeepdive.org/>). This record is also normalized to the yearly count of papers that contain the word ‘stratigraphy’ (red, right y-axis), and shows that the acceleration in rate of published $\delta^{13}\text{C}$ chemostratigraphy papers is not driven solely by a general growth in stratigraphic research. In both records, an uptick in the early 1970’s is apparent, coincident with the initiation of the Deep Sea Drilling Program Data in 1968.

39 they formed. Of singular importance is the observation that modern shallow-water depositional
 40 systems are dominated by local carbon cycling, leading to large differences between the carbon
 41 isotope composition of modern, shallow-water CaCO_3 sediment and average carbonate burial.
 42 Understanding this disconnect is important, because all sediments older than ~ 200 million years
 43 old formed in analogous environments, as abyssal sediments are recycled and destroyed due to
 44 seafloor spreading and subduction. Disentangling the mixture of global and local control in
 45 modern carbon isotope values is therefore vital for the interpretation of deep time records, and
 46 for the basis of carbon isotope chemostratigraphy.

47

48 2 Systematics of carbon isotope chemostratigraphy

49 2.1 Development and history

50 The groundwork for carbon isotope chemostratigraphy was laid by the pioneering research in
 51 isotope geochemistry by Alfred Nier (Nier and Gulbransen 1939) and Harold Urey (Urey et al.
 52 1936; Urey 1947). Both made the earliest measurements of the ratios of carbon isotopes in

53 natural materials by mass spectrometry (Fig. 1A). By convention, rather than discussing such
54 values as simple ratios (e.g., $^{13}R = \frac{^{13}C}{^{12}C}$), carbon isotopic values are expressed in the δ -notation
55 relative to a common standard (V-PDB, Craig 1953):

$$\delta^{13}C = \left(\frac{^{13}R_{sample}}{^{13}R_{standard}} - 1 \right) \times 10^3 \quad (1)$$

56 With regards to chemostratigraphy, one of most important early findings was that organic matter
57 is depleted in ^{13}C relative to carbonate minerals (Nier and Gulbransen 1939). This discovery
58 forms the backbone of all studies using $\delta^{13}C$ values to study the carbon cycle in deep time. The
59 first long-term record of Phanerozoic carbonate $\delta^{13}C$ values was published in 1964 (Keith and
60 Weber 1964), followed by the first continuous Precambrian record in 1975 (Schidlowski et al.
61 1975), both records remarking on the apparent lack of long-term variability in $\delta^{13}C$ values.
62 These observations led to the prevailing hypothesis that the burial of organic carbon (and con-
63 sequentially, atmospheric oxygen levels) have been relatively stable throughout the Phanerozoic
64 (Broecker 1970).

65 The later development of $\delta^{13}C$ measurements as a tool for stratigraphic correlation is closely
66 linked to the initiation of the Deep Sea Drilling Program (1968–1983, Fig. 1A). Following the
67 success of using $\delta^{18}O$ for correlation in Pleistocene and Pliocene deep sea sediment cores, car-
68 bon isotope stratigraphy was first used in the late 1970's (Fig. 1B), based on the observation
69 of reproducible and coherent changes in $\delta^{13}C$ values of carbonate (excursions of $\sim -0.5\text{\textperthousand}$) in
70 Miocene sediments across the Pacific Ocean (Loutit and Kennett 1979; Keigwin and Shackleton
71 1980). Contemporaneous with these developments, the observation of significant short term
72 fluctuations – excursions – of carbonate $\delta^{13}C$ values in Cretaceous sedimentary rocks, associ-
73 ated with ocean anoxic events (OAEs), pushed the use of carbon isotope stratigraphy into older
74 portions of the geologic record (Scholle and Arthur 1980). Today, numerous $\delta^{13}C$ records from
75 Cenozoic deep marine sediment cores have demonstrated systematic variations across the globe
76 that correlate with major climatic events, used for global correlation and age model construc-
77 tion (e.g., Westerhold et al. 2020).

79

80 2.2 One-box model of the carbon cycle

81 At its core, carbon isotope chemostratigraphy builds on the assumption that the $\delta^{13}C$ values
82 of carbonate ($\delta^{13}C_{carb}$) reflect the $\delta^{13}C$ values of dissolved inorganic carbon ($\delta^{13}C_{DIC}$, Fig. 2)
83 in a well-mixed ocean in equilibrium with the atmosphere (Kump and Arthur 1999). In this
84 view, independent of geographic location, all carbonate precipitated and deposited has the same
85 value, and excursions in $\delta^{13}C_{carb}$ will be synchronous and useful as stratigraphic tie-points be-
86 tween and within sedimentary basins.

87

88 The $\delta^{13}C_{DIC}$ values of a well-mixed ocean in equilibrium with the atmosphere are set by the
89 relative sizes and isotopic values of carbon sources and sinks. The primary sources of carbon to
90 the system are weathering (F_w), metamorphism and volcanic outgassing (F_{volc}), while the sinks
91 are burial of organic carbon ($F_{b,org}$) and carbonate ($F_{b,carb}$), with each flux carrying a (poten-
92 tially) predictable isotopic value (Kump and Arthur 1999). Most commonly, the $\delta^{13}C$ value of
93 CO₂ from volcanic and metamorphic outgassing is assumed to reflect the isotopic composition
94 of the mantle ($\sim -5\text{\textperthousand}$), the $\delta^{13}C_{carb}$ value is assumed to be equal to the composition of seawater,
95 and the $\delta^{13}C_{org}$ value is assumed to be depleted in ^{13}C by approximately $\sim 25\text{\textperthousand}$ relative to
96 $\delta^{13}C_{carb}$ (Kump and Arthur 1999; Hayes et al. 1999).

97

98 Based on the simple framework outlined above, mathematical expressions can be written for
99 carbon mass (M) and carbon isotope (δ_{DIC}) balance in the ocean-atmosphere system (Fig. 2).

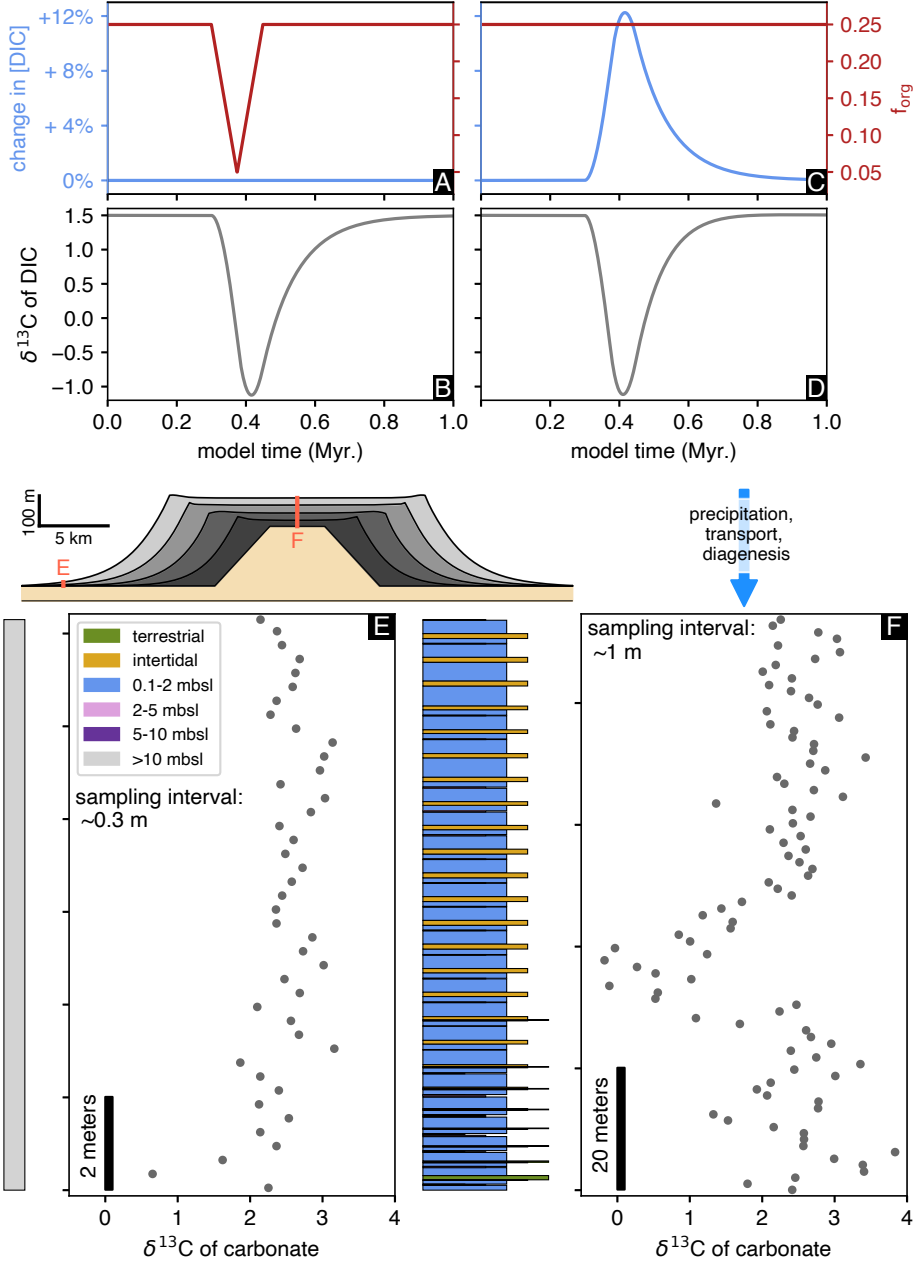


Figure 2: Toy demonstrations of carbon cycle perturbations that can be modeled using equation 5 (see section 2.2), and how these perturbations might be recorded in shallow water carbonate strata. **(A, B)** A transient decrease in the relative burial flux of organic carbon will result in a negative excursion in $\delta^{13}\text{C}$ values of DIC. If CO_2 input to the ocean-atmosphere is increased via oxidation of organic carbon, the amount of DIC would increase (**C**) and an identical negative excursion can be produced (**D**), but with a very different driver than in **(A, B)**. How these seawater signals are recorded in sediments is explored with a simple numerical model of a shallow-water carbonate platform, with CaCO_3 sediment production on the platform edges (e.g., fringing reefs), which is then transported via hillslope diffusion. As the platform aggrades and progrades, the proscribed $\delta^{13}\text{CDIC}$ signal from **(B)** or **(D)** is recorded with a fractionation of 1‰ and added “geological noise” (e.g., effects from differential mineralogy, organic matter respiration, etc.). In distal settings (**E**), where all sedimentation occurs in depths >10 meters below sea-level (mbsl), accumulation rates are low and carbon cycle perturbations are captured poorly even with dense stratigraphic sampling. In platform interior settings (**F**), accumulation rates are higher, and the resulting $\delta^{13}\text{C}_{\text{carb}}$ record is expanded.

100 The change in the mass of carbon in the system through time ($\frac{dM}{dt}$) equals the balance between
 101 sources and sinks:

102

$$\frac{dM}{dt} = F_w + F_{volc} - F_{b,org} - F_{b,carb} \quad (2)$$

103 By the same logic, isotope mass balance can be treated if each flux or reservoir is multiplied by
 104 its respective $\delta^{13}\text{C}$ value:

$$\frac{dM\delta_{DIC}}{dt} = \delta_w F_w + \delta_{volc} F_{volc} - \delta_{org} F_{b,org} - \delta_{carb} F_{b,carb} \quad (3)$$

105

106

107 By rearranging these equations using the product rule of calculus ($dM\delta/dt = M * d\delta/dt + \delta * dM/dt$), it is possible to isolate $d\delta/dt$ and derive a time-dependent differential equation for
 108 ocean $\delta^{13}\text{C}_{DIC}$ values:

$$\frac{d\delta_{DIC}}{dt} = \frac{F_w(\delta_w - \delta_{DIC}) + F_{volc}(\delta_{volc} - \delta_{DIC}) - F_{b,org}(\delta_{b,org} - \delta_{DIC}) - F_{b,carb}(\delta_{b,carb} - \delta_{DIC})}{M} \quad (4)$$

110 This expression typically is simplified further by making three assumptions (Kump and Arthur
 111 1999). First, the $\delta^{13}\text{C}$ value of carbonate is set equal to the value of DIC ($\delta_{DIC} = \delta_{carb}$). Second,
 112 the input fluxes from weathering and volcanic outgassing are merged into a single input flux
 113 from rivers (F_{riv}). Third, the $\delta^{13}\text{C}$ value of organic carbon is defined by an average offset from
 114 carbonate ($\Delta_B = \delta_{org} - \delta_{carb}$). We explore the validity of these assumptions in more detail
 115 below (section 3), but they can be used to simplify equation 4 to:

$$\frac{d\delta_{carb}}{dt} = \frac{F_{riv}(\delta_{riv} - \delta_{carb}) - F_{b,org} * \Delta_B}{M} \quad (5)$$

116 This box model approach (equation 5) shows that the $\delta^{13}\text{C}$ value of the global ocean (and, by
 117 extension, that of buried marine carbonate) may evolve with time through numerous forcings,
 118 with different processes often generating the same δ_{carb} time series. For example, total carbon
 119 input (F_{riv}) and burial ($F_{b,carb} + F_{b,org}$) fluxes can remain equal, while the ratio of $F_{b,org}$ relative
 120 to $F_{b,carb}$ may decrease. In this scenario, M will remain the same but $\delta^{13}\text{C}$ of DIC will fall
 121 (Fig. 2A–B). Transient imbalances in the mass fluxes of carbon can lead to changes in both M
 122 and $\delta^{13}\text{C}_{DIC}$: oxidation of a large pool of organic carbon ($\delta^{13}\text{C} \approx -25\text{\textperthousand}$) will increase ocean
 123 DIC concentration and will lower its $\delta^{13}\text{C}$ value (Fig. 2C–D).

124

125 When considering time scales much longer than the residence time of carbon in the ocean-
 126 atmosphere system ($>10^5$ years), the carbon cycle box model is in a steady state, and the input
 127 and output mass fluxes must balance each other. In this scenario, equation 5 can be further
 128 simplified by setting $d\delta_{carb}/d\delta_t = 0$ and setting the input flux of carbon equal to the burial
 129 fluxes ($F_{riv} = F_{b,org} + F_{b,carb}$):

130

$$\frac{F_{org}}{F_{org} + F_{carb}} = \frac{\delta_{riv} - \delta_{carb}}{\Delta_B} = f_{org} \quad (6)$$

131 The burial fraction of organic carbon (F_{org}) relative to total carbon burial ($F_{org} + F_{carb}$) is com-
 132 monly abbreviated in the literature as f_{org} (Fig. 2A and C). Equation 6 demonstrates that if we
 133 know both the average isotope offset between organic matter and carbonate (e.g., $\Delta_B = -25\text{\textperthousand}$,
 134 Hayes et al. 1999) and the average isotopic value of the carbon input flux (δ_{riv} , assumed to equal
 135 the mantle value of $\sim -5\text{\textperthousand}$), then it is possible to calculate f_{org} (Kump and Arthur 1999). By

136 illustration, if δ_{carb} is set to the modern DIC value of $\sim 0\text{\textperthousand}$, then f_{org} is 0.2, implying that on
137 Earth today 20% of the carbon sink is organic carbon burial and 80% is carbonate burial.

138
139 This hypothesis that $\delta^{13}\text{C}_{carb}$ values can be directly linked to oxygen production by estimating
140 the relative burial flux of organic carbon (f_{org}) is widely used to interpret deep time $\delta^{13}\text{C}_{carb}$
141 records, both in the Precambrian (e.g., Knoll et al. 1986; Kaufman et al. 1997; Canfield et
142 al. 2020) and Phanerozoic (e.g., Broecker 1970; Saltzman 2005; Berner 2006). To apply this
143 framework, it is assumed that $\delta^{13}\text{C}_{carb}$ values measured across several stratigraphic columns
144 are representative of the average carbonate burial sink and that stratigraphic trends in $\delta^{13}\text{C}_{carb}$
145 represent secular changes in the global carbon cycle. Below we examine this assumption more
146 closely. Specifically, we investigate the effects of local isotopic variability on stratigraphic records
147 of $\delta^{13}\text{C}_{carb}$ and the implications for global mass balance.

148

149 **3 Local controls and issues of fidelity and diagenesis**

150 In theory, according to the model frame work developed above, time series of $\delta^{13}\text{C}$ values of
151 either carbonate or organic carbon can be used to reconstruct global ocean $\delta^{13}\text{C}_{DIC}$ values. In
152 practice, $\delta^{13}\text{C}$ of carbonate ($\delta^{13}\text{C}_{carb}$) are far more common, owing in large part to the high
153 throughput capabilities of sample preparation and modern instrumentation. When interpreting
154 $\delta^{13}\text{C}$ records in terms of the global carbon cycle (e.g., equations 5 and 6), the important question
155 is: does the record capture a representative $\delta^{13}\text{C}$ value of average carbonate burial? For Ceno-
156 zoic deep-marine $\delta^{13}\text{C}$ records, datasets can be collected that cover large geographical areas of
157 the deep ocean sea floor and, when stacked in time bins, are likely to satisfy this constraint
158 (e.g., Westerhold et al. 2020). By contrast, the chemostratigraphic records from shallow-water
159 settings, such as carbonate platforms or epeiric seas, are complicated by a much larger range in
160 $\delta^{13}\text{C}_{carb}$ values owing to local carbon cycling (Fig. 3, Holmden et al. 1998).

161

162 Today, it is accepted that the average $\delta^{13}\text{C}_{carb}$ value of carbonate forming on shallow-water
163 platforms does not represent the $\delta^{13}\text{C}_{carb}$ value of average carbonate burial, even when inte-
164 grated across the globe (Swart 2008). Prior to the evolution of a deep-marine carbonate sink in
165 the mid-Mesozoic, carbonate platforms likely played a bigger role in the global carbonate burial
166 budget (Opdyke and Wilkinson 1988), meaning that average platform $\delta^{13}\text{C}_{carb}$ would have been
167 closer (or equal) to globally average carbonate $\delta^{13}\text{C}$. As a result, following the approach from
168 the Cenozoic, a hypothesis for the pre-Mesozoic is that changes in the global carbon cycle can
169 be evaluated by collecting correlative chemostratigraphic records of $\delta^{13}\text{C}$ values across several
170 continents. However, even when independent tools such as biostratigraphy or geochronology
171 are available for correlation, the timescales for perturbations to the global carbon cycle ($<10^5$
172 years, Fig. 2A–D) are challenging to resolve for even the best chronostratigraphic age models
173 (Schoene 2014; Holland 2020), especially for pre-Mesozoic strata.

174

175 Thus, if shallow-water carbon successions are only broadly correlative (e.g., at the 0.5–5 million
176 year level), or only recorded in a subset of basins globally, apparent excursions in $\delta^{13}\text{C}_{carb}$ val-
177 ues could easily represent local processes rather than global perturbations (Fig. 2E,F). Given
178 these uncertainties, how variability in $\delta^{13}\text{C}$ values in shallow-water environments can be ex-
179 pressed in stratigraphic records on local, regional, and global scales is vitally important for
180 $\delta^{13}\text{C}$ chemostratigraphy (Fig. 3).

181 **3.1 Local variability in carbon sources and sinks**

182 **Riverine input:** One of the main sources of DIC to shallow-water environments is the dis-
183 charge of rivers and groundwater to coastal settings (Fig. 3). Contrary to the assumptions
184 made above, concerning a single isotopic value for riverine input (F_{riv} , equation 5–6), there

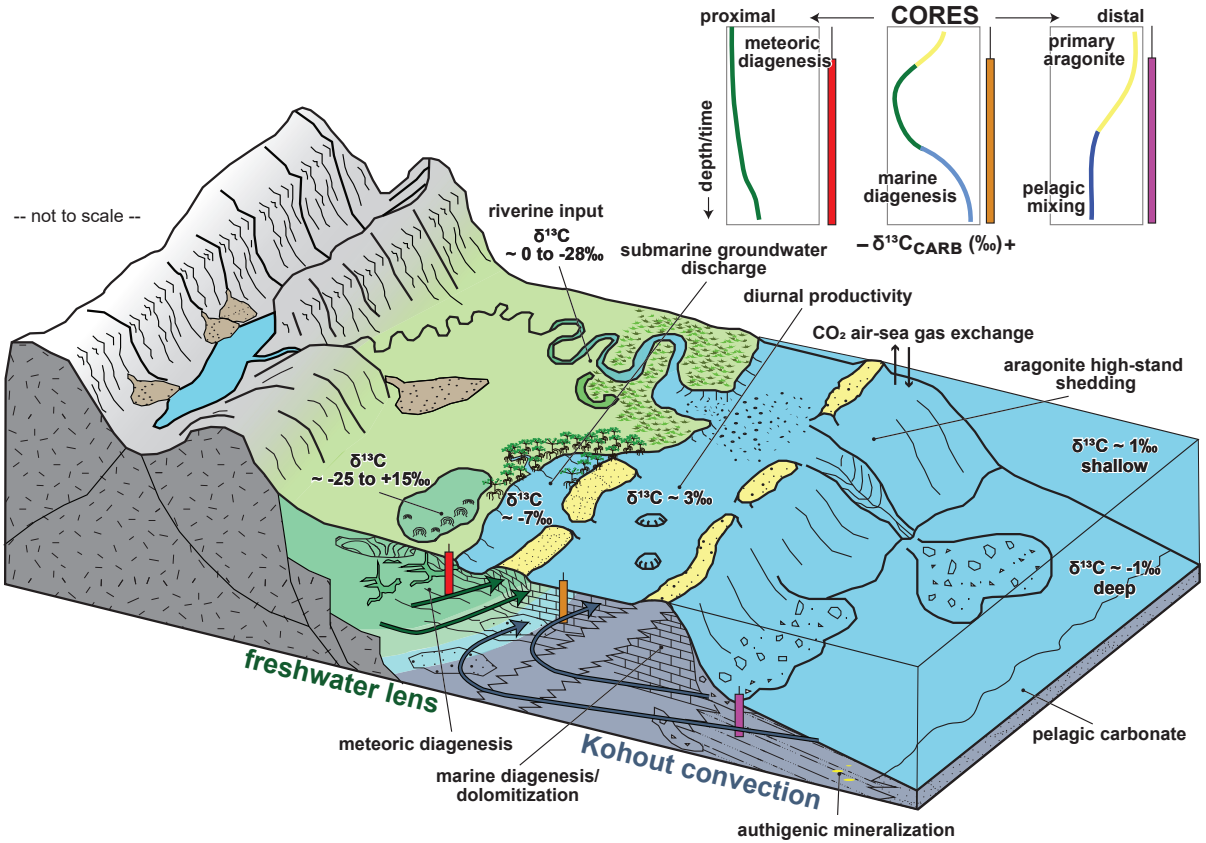


Figure 3: Schematic illustrating the variability in surface water $\delta^{13}\text{C}$ across different depositional environments in carbonate platform or epeiric sea settings (see text in section 3 for description of each environment). Values of $\delta^{13}\text{C}$ refer to dissolved inorganic carbon (DIC), unless stated otherwise. Core profiles illustrate the coincident variability in bulk carbonate $\delta^{13}\text{C}$ that can be expected as products of local surface water chemistry and carbonate diagenesis.

185 is a large range in the concentration and isotopic composition of DIC from rivers (even if the
 186 average value is well constrained). As one example, streams in Sweden yielded $\delta^{13}\text{C}_{\text{DIC}}$ values
 187 ranging between -28 to 0‰ (Campeau et al. 2017). This range is a product of upstream soil
 188 respiration, local mixtures of carbonate and organic carbon weathering, and variable degrees
 189 of stream water DIC equilibration with atmospheric CO_2 . In general, rivers with low $\delta^{13}\text{C}_{\text{DIC}}$
 190 values often are associated with siliciclastic-dominated catchments with high degrees of organic
 191 carbon respiration, while higher $\delta^{13}\text{C}_{\text{DIC}}$ values often are associated with carbonate-dominated
 192 catchments (Khadka et al. 2014).

193
 194 The difference in $\delta^{13}\text{C}_{\text{DIC}}$ values between siliciclastic- and carbonate-dominated rivers may be
 195 important to consider when interpreting the stratigraphic trends of $\delta^{13}\text{C}_{\text{carb}}$ in mixed carbonate-
 196 siliciclastic depositional systems (e.g., Rodriguez Blanco et al. 2020). On carbonate platforms,
 197 adjacent to continental blocks, deposition is influenced by the clastic sediment and nutrient
 198 influx from river drainage systems that migrate over time. The chemostratigraphic implications
 199 of such a depositional setting is that $\delta^{13}\text{C}$ values of carbonate that precipitates in coastal waters
 200 may vary as a function of local siliciclastic input. It may be possible to disentangle this effect
 201 by linking sedimentological facies observations with $\delta^{13}\text{C}_{\text{carb}}$ values (Rodriguez Blanco et al.
 202 2020). However, while the influx of siliciclastic material largely is controlled by local fluvial-
 203 deltaic processes, it is possible that global climate and/or eustatic sea-level change can generate
 204 widespread changes in relative weathering of carbonate versus siliciclastic material (Harper et al.

205 2015). For example, increased weathering and diagenesis of carbonate platforms during glacial
206 sea-level lowstands would likely increase the $\delta^{13}\text{C}$ value of global riverine inputs (Kump et al.
207 1999; Dyer et al. 2015). Alternatively, increased weathering and remineralization of organic-rich
208 sediments may increase the input flux of ^{13}C depleted carbon and decrease the surface ocean
209 $\delta^{13}\text{CDIC}$ value (Fig. 2C,D). While possibly global in scale, the impact of changes in riverine
210 weathering fluxes are easily amplified in shallow-water platforms and epeiric seas (e.g., Holmden
211 et al. 1998).

212 **Submarine groundwater discharge:** In addition to riverine input, submarine ground-
213 water discharge also has measurable effects on surface water $\delta^{13}\text{CDIC}$ values in coastal areas
214 (Fig. 3). For example, in Florida Bay and the Little Bahama Banks, submarine groundwa-
215 ter discharge leads to surface water $\delta^{13}\text{CDIC}$ values down to $-7\text{\textperthousand}$ (Patterson and Walter 1994).
216 These low values are a product of organic carbon respiration in the freshwater aquifer that flows
217 towards the sea from platform interiors. In some coastal areas, such as in mangrove-dominated
218 tidal creeks and reefs, the flux of groundwater discharge varies with the tides, with the highest
219 inputs of groundwater at low tide, which results in high creek DIC concentrations (>3 mmol/kg,
220 Maher et al. 2013). Surface water $\delta^{13}\text{CDIC}$ values vary by up to $10\text{\textperthousand}$ across a tidal cycle, from
221 $-8\text{\textperthousand}$ at low tide to $+2\text{\textperthousand}$ at high tide (Maher et al. 2013). However, it is unlikely that the
222 entire range in $\delta^{13}\text{CDIC}$ is captured by carbonate precipitation, as the carbonate saturation
223 state ($\Omega = \{Ca^{2+}\} * \{CO_3^{2-}\} / K_{sp}$, where K_{sp} is the solubility product for aragonite) is also
224 lowered with the input of respired and dissolved CO_2 , thus predicting less precipitation during
225 periods of high submarine groundwater discharge and low $\delta^{13}\text{CDIC}$.

226 Despite the potential lack of carbonate mineral precipitation at times of very low $\delta^{13}\text{CDIC}$,
227 stratigraphic records from carbonate platforms may still preserve $\delta^{13}\text{C}_{carb}$ signals that are mod-
228 ified by local submarine groundwater discharge. For example, if local discharge into coastal
229 environments carries significant amounts of dissolved carbonate in solution, positive $\delta^{13}\text{C}$ ‘ex-
230 cursions’ can be created in carbonate precipitating from these waters (Holmden et al. 2012).

232 **Diurnal productivity:** Dissolved inorganic carbon in coastal areas can exhibit large diurnal
233 fluctuations in $\delta^{13}\text{CDIC}$ values, driven by day-time photosynthesis and night-time respiration
234 of organic matter (Fig. 3). For example, surfaces waters in reefs on O’ahu show a range in
235 $\delta^{13}\text{CDIC}$ values of up to 5\textperthousand across a diurnal cycle (Richardson et al. 2017). In such settings,
236 carbonate precipitation occurs predominantly during the most productive parts of the diurnal
237 cycle, recording $\delta^{13}\text{C}_{carb}$ values up to $+7\text{\textperthousand}$ in platform aragonite (Geyman and Maloof 2019).
238 This pattern is due to the respiration of organic carbon at night-time, lowering Ω and hindering
239 carbonate precipitation. As a result, stratigraphic records from shallow-water environments
240 may be biased towards higher $\delta^{13}\text{C}_{carb}$ values relative to average surface water $\delta^{13}\text{CDIC}$. If
241 shallow platforms contribute significantly to the global carbon budget then, as the relative area
242 of shallow shelves increases, the burial of ^{13}C -enriched carbonate will lower the average seawater
243 $\delta^{13}\text{CDIC}$ to satisfy global mass balance (Geyman and Maloof 2019).

244 **Air-sea gas-exchange:** Highly variable $\delta^{13}\text{CDIC}$ values of shallow-water environments are
245 possible due to slow rates of air-sea gas exchange, meaning that surface water $\delta^{13}\text{CDIC}$ can
246 diverge from equilibrium values with the overlying atmosphere (Lynch-Stieglitz et al. 1995).
247 The exchange of CO_2 across the air-sea interface is also associated with kinetic isotope effects,
248 with the preferential dissolution and degassing of ^{12}C (e.g., Wanninkhof 1985). Surface waters
249 that have low DIC concentrations with net CO_2 invasion may therefore have lower $\delta^{13}\text{CDIC}$
250 values compared to surface waters with high DIC concentration and net CO_2 degassing (Wan-
251 ninkhof 1985). The isotope effects of air-sea gas exchange can dampen the $\delta^{13}\text{CDIC}$ enrichment
252 from the biological pump in surface waters, but in the modern ocean these kinetic effects are

253 relatively small, leading to spatial variability in surface waters $\delta^{13}\text{C}_{\text{DIC}}$ of the open ocean of
254 up to 2‰ (Lynch-Stieglitz et al. 1995)

255

256 In contrast to the modern surface-ocean, kinetic isotope effects associated with CO_2 exchange
257 can be pronounced in hypersaline and restricted environments (e.g., Lazar and Erez 1992; Clark
258 et al. 1992; Beeler et al. 2020). In these settings, carbonate with $\delta^{13}\text{C}$ values between -25 and
259 +15‰ have been documented (Fig. 3), with rapid invasion of CO_2 leading to low $\delta^{13}\text{C}_{\text{carb}}$
260 values (Clark et al. 1992) and degassing of CO_2 leading to high $\delta^{13}\text{C}_{\text{carb}}$ values (Beeler et al.
261 2020). It is unclear if kinetic effects are expressed in stratigraphic $\delta^{13}\text{C}_{\text{carb}}$ records, but it has
262 been suggested that these processes may have been more pronounced in Precambrian platform
263 environments, where abiotic or microbially-mediated carbonate precipitation likely was more
264 important (Ahm et al. 2019; Husson et al. 2020).

265 **Redox and authigenic mineralization:** In both shallow and deep marine settings, $\delta^{13}\text{C}_{\text{carb}}$
266 values may be influenced by anoxic remineralization of organic carbon and consequent precipi-
267 tation of in-situ (authigenic) carbonate in the sediment pore-space (Fig. 3). More specifically,
268 methanogenesis (methane production) and sulfate reduction within the sediment pile may lead
269 to the precipitation of authigenic carbonate with extreme $\delta^{13}\text{C}_{\text{carb}}$ values. Methane (CH_4) has
270 very low $\delta^{13}\text{C}$ values (-60 to -80‰, Claypool and Kaplan 1974), meaning that its produc-
271 tion leaves residual porewater DIC with heavy $\delta^{13}\text{C}$ values. In contrast to oxic respiration of
272 organic matter, which lowers pore-water Ω values and promotes carbonate dissolution, anoxic
273 respiration (such as sulfate reduction) tends to increase Ω and rates of carbonate precipitation
274 (Claypool and Kaplan 1974). For example, methane oxidation by sulfate reduction has been
275 shown to produce carbonate cements with $\delta^{13}\text{C}_{\text{carb}}$ values down to -56‰ (Hovland et al. 1987).
276 In contrast, $\delta^{13}\text{C}_{\text{carb}}$ values up to +16‰ has been documented in stromatolitic and microbial
277 carbonate as the result of methanogenesis (Birgel et al. 2015). However, whether authigenic car-
278 bonate formation is a significant carbonate sink with the potential to influence global $\delta^{13}\text{C}_{\text{DIC}}$
279 values has been a source of debate throughout the last decade (Bjerrum and Canfield 2004;
280 Higgins et al. 2009; Schrag et al. 2013; Canfield et al. 2020).

281 3.2 Carbonate mineralogy, fractionation, and mixing

282 The $\delta^{13}\text{C}$ value of carbonate is fractionated relative to local surface water DIC, with the prefer-
283 ential uptake of ^{13}C into the carbonate mineral lattice (contrary to the assumption in equation
284 5 that $\delta_{\text{DIC}} = \delta_{\text{carb}}$). The magnitude of fractionation varies for different carbonate polymorphs.
285 Aragonite is more enriched in ^{13}C (~3‰) compared to calcite (~1‰, Romanek et al. 1992).
286 As a result, stratigraphic changes in δ_{carb} can be produced by the mixing of aragonite, which is
287 predominantly made in shallow-water carbonate factories like The Bahamas (Lowenstam and
288 Epstein 1957), and calcite, the dominant polymorph of pelagic calcifiers (Bown et al. 2004).
289 For example, it is possible to generate systematic changes in the relative fractions of platform
290 versus pelagic derived carbonate during periods of sea-level change, which may lead to coherent
291 and reproducible stratigraphic changes in $\delta^{13}\text{C}$ values that are decoupled from changes to the
292 global carbon cycle (see Case Study below, Swart and Eberli 2005; Swart 2008). Mixing of
293 calcite and aragonite end-members, even if both formed from the same fluid and DIC pool, can
294 also lead to “noise” in the stratigraphic $\delta^{13}\text{C}_{\text{carb}}$ record (e.g., Fig. 2E,F).

295

296 In addition to the mineralogical differences in carbon isotope fractionation, there is considerable
297 variability in isotopic values of organic matter and, hence, local differences in Δ_B (equations 5
298 and 6, Hayes et al. 1999). The range of isotopic values of organic matter are related to organ-
299 ismal growth rates and the specific carbon fixation pathways employed (Pearson 2010). First,
300 species-specific fractionation results in a large isotopic range where, for example, terrigenous,
301 coastal, and marine organic carbon can be offset by up to 20‰ (Oehlert et al. 2012). Second,

302 the net fractionation factor between local surface water DIC and organic carbon (Δ_B) is de-
303 pendent upon the concentration of CO₂ in the ambient environment (Popp et al. 1998), with
304 higher CO₂ levels leading to a more negative fractionation (reflecting preferential uptake of
305 ¹²C). These isotope effects are relevant to consider in shallow-water coastal environments where
306 DIC concentrations (and hence ambient CO₂) vary on semi-diurnal and diurnal timescales (see
307 above).

308 Differences in isotopic fractionation of organic matter can be recorded by chemostratigraphy,
309 since the bulk isotopic composition of organic carbon at a given locality will reflect the relative
310 input of different sources (Fig. 3). In coastal environments, especially, these inputs can be
311 highly variable both in space and time, with transport and deposition of sediments from coastal
312 environments into deeper waters causing stratigraphic changes in $\delta^{13}\text{C}$ values of both carbonate
313 and organic carbon due to mixing (Oehlert et al. 2012; Oehlert and Swart 2014).

315

316 3.3 Carbonate diagenesis

317 As carbonate sediments are buried and lithified, they pass through several stages of diagenesis
318 (e.g., meteoric, marine, burial), where primary metastable carbonate minerals dissolve and di-
319 agenetic minerals precipitate. The most common approach for predicting whether the isotopic
320 value of given element (e.g., C, O, Ca, trace metals) will be reset during lithification is to con-
321 sider the comparative abundances of that element in altering fluids and in the sediment (Banner
322 and Hanson 1990). If an element has low abundance in the fluid relative to the sediment (such
323 as for carbon in seawater compared to CaCO₃ sediment), the sediment is more likely to retain
324 its original isotopic composition (sediment-buffered diagenesis). However, in settings with high
325 fluid flow rates (advection dominated), the cumulative fluid-to-rock ratio for carbon becomes
326 high and the isotopic composition of the primary carbonate sediment can be reset (fluid-buffered
327 diagenesis). Fluid-buffered diagenetic regimes are common in shallow-water and peri-platform
328 environments where flow rates are high and largely driven by buoyancy and geothermal convec-
329 tion (Fig. 3, ~10 cm/yr, Henderson et al. 1999; Kohout 1965). In contrast, sediment-buffered
330 diagenesis occurs in settings where fluid flow rates are low (diffusion dominated) or in settings
331 with low fluid carbon concentrations. During sediment-buffered diagenesis, the isotopic compo-
332 sition of the pore-fluid is in equilibrium with the sediment and does not have the potential to
333 alter $\delta^{13}\text{C}_{\text{carb}}$ values. Sediment-buffered diagenesis is characteristic of the deep ocean seafloor
334 where subsurface fluid flow is diffusion dominated (e.g., Fantle et al. 2010) or during late-stage
335 burial diagenesis where pore-fluid tends to have reacted extensively with the host strata. As a
336 result, if $\delta^{13}\text{C}$ values are reset, this process likely occurs relatively early, within the first 100s
337 meter below the seafloor, at burial temperatures <40°C (Staudigel and Swart 2019; Murray
338 et al. 2021).

339

340 **Calcium isotopes:** Other geochemical proxies can be measured along with $\delta^{13}\text{C}_{\text{carb}}$ to eval-
341 uate the degree of diagenetic alteration (e.g., carbonate $\delta^{18}\text{O}$ and Mn/Sr measurements). More
342 recently, calcium isotopes ($\delta^{44}/{}^{40}\text{Ca}$) has emerged as a powerful tool for disentangling the de-
343 gree of fluid versus sediment-buffered diagenesis of $\delta^{13}\text{C}_{\text{carb}}$ values. The advantage of carbonate
344 $\delta^{44}/{}^{40}\text{Ca}$, in comparison to $\delta^{18}\text{O}$ values for example, is that the ratio of calcium in carbonate
345 minerals relative to seawater is similar to that of carbon, which means that the two isotopic sys-
346 tems respond to diagenesis at similar fluid-to-rock ratios (Fantle and Higgins 2014; Ahm et al.
347 2018). Combining $\delta^{13}\text{C}_{\text{carb}}$ values with both $\delta^{44}/{}^{40}\text{Ca}$ and Sr/Ca ratios can fingerprint different
348 diagenetic end-members (Fig. 4C–D). This tool is useful because Ca isotope fractionation and Sr
349 partitioning is sensitive to both carbonate mineralogy and precipitation rate (Tang et al. 2008;
350 Gussone et al. 2005). Primary aragonite is more depleted in ⁴⁴Ca and enriched in Sr (with values

351 of $-1.5\text{\textperthousand}$ and 10 mmol/mol, respectively) relative to primary calcite ($-1\text{\textperthousand}$ and ~ 1 mmol/mol).
352 Diagenetic calcite or dolomite is characterized by lower Sr contents (<1 mmol/mol) and less
353 fractionated $\delta^{44/40}\text{Ca}$ values, approaching $\sim 0\text{\textperthousand}$ at equilibrium with the pore-fluids (Fantle and
354 DePaolo 2007; Jacobson and Holmden 2008). As a result, sediment-buffered diagenesis will be
355 labeled by low $\delta^{44/40}\text{Ca}$ values and relatively high Sr/Ca ratios, while fluid-buffered diagenesis will be
356 labeled by high $\delta^{44/40}\text{Ca}$ values and low Sr/Ca ratios (Fig. 4C–D, Higgins et al. 2018).

357

358 In addition to helping identify primary and diagenetic end-members, $\delta^{44/40}\text{Ca}$ values can also
359 shed light on the degree to which geographically disparate carbonate successions, which often
360 are correlated using carbon isotope chemostratigraphy (especially in the Precambrian), reflect
361 the globally-averaged carbonate sink (Blättler and Higgins 2017). The main Ca^{2+} sink from the
362 ocean is the burial of carbonate. Thus, a prediction for the global calcium cycle is that when
363 in a steady state, the globally-averaged calcium isotope composition of carbonate sediments
364 should equal that of bulk silicate Earth ($\sim -1\text{\textperthousand}$ on time-scales $>10^6$ years, Skulan et al. 1997;
365 Blättler and Higgins 2017). In other words, if the Ca cycle is in steady state, the $\delta^{44/40}\text{Ca}$ of
366 the average carbonate sink has a predictable value ($\sim -1\text{\textperthousand}$). Calcium isotopes can therefore be
367 used not only to understand diagenesis, but when averaged across the global, may also be used
368 to evaluate if correlated stratigraphic sections reflect the average carbonate burial sink. For
369 example, in scenarios where negative $\delta^{13}\text{C}$ values correlate with $\delta^{44/40}\text{Ca}$ values more negative
370 than bulk silicate Earth across several stratigraphic sections, mass balance requires that other
371 carbonate sinks must exist that record more positive $\delta^{44/40}\text{Ca}$ values (e.g., authigenic cements,
372 hydrothermal veins, or dolomitized carbonate platforms, Gussone et al. 2020). While it is not
373 necessary that the $\delta^{13}\text{C}$ values of these unmeasured carbonates also are positive, it is uncertain
374 that the globally-average carbonate sink does have a negative $\delta^{13}\text{C}$ value, and these values
375 do not need to be tracking the global carbon cycle. The alternative scenario, where several
376 stratigraphic sections with negative $\delta^{13}\text{C}$ values also coincide with an average $\delta^{44/40}\text{Ca}$ value
377 of $\sim -1\text{\textperthousand}$, strengthens the argument for interpreting carbon isotope values in terms of global
378 carbon fluxes (e.g., Fig. 2A–D).

379

380 On shorter time scales, within the residence time of calcium in the ocean ($<10^6$ years), it is pos-
381 sible to have excursions in $\delta^{44/40}\text{Ca}$ values that reflect transient imbalances in calcium inputs
382 and outputs. In this scenario, it is possible to have $\delta^{13}\text{C}$ and $\delta^{44/40}\text{Ca}$ excursions that cor-
383 relate across the globe. Numerical models that include the coupled carbon- CaCO_3 cycle have
384 demonstrated that the maximum transient $\delta^{44/40}\text{Ca}$ excursion that can occur from the combined
385 effects of increased weathering (which can increase global ocean Ca concentration) and ocean
386 acidification (which can depress CaCO_3 burial) is $\sim -0.3\text{\textperthousand}$ (Komar and Zeebe 2016). There
387 are two implications for carbon isotope chemostratigraphy. First, if a $\delta^{13}\text{C}$ excursion correlates
388 with a $\delta^{44/40}\text{Ca}$ excursion, then the duration of these excursions must be $<10^6$ years (if Ca
389 residence time is similar to the modern). Second, the magnitude of change in $\delta^{44/40}\text{Ca}$ values
390 has to be $<0.3\text{\textperthousand}$. If either is not true, then the excursions are difficult to interpret in terms of
391 the global C and Ca cycles, indicating that local controls are most important for $\delta^{44/40}\text{Ca}$ and
392 $\delta^{13}\text{C}$ values (Fig. 3).

393

394 In the next section, we highlight case-studies that demonstrate the potential to disentangle
395 global and local processes using a combination of carbonate $\delta^{44/40}\text{Ca}$ and $\delta^{13}\text{C}$ values.

396

397 4 Case studies

398 4.1 The Great Bahamas Bank

399 The Bahamas Drilling Project and the Ocean Drilling Program (ODP Leg 166), acquired a
400 transect of cores across the Great Bahamas Bank west of Andros Island, including the platform

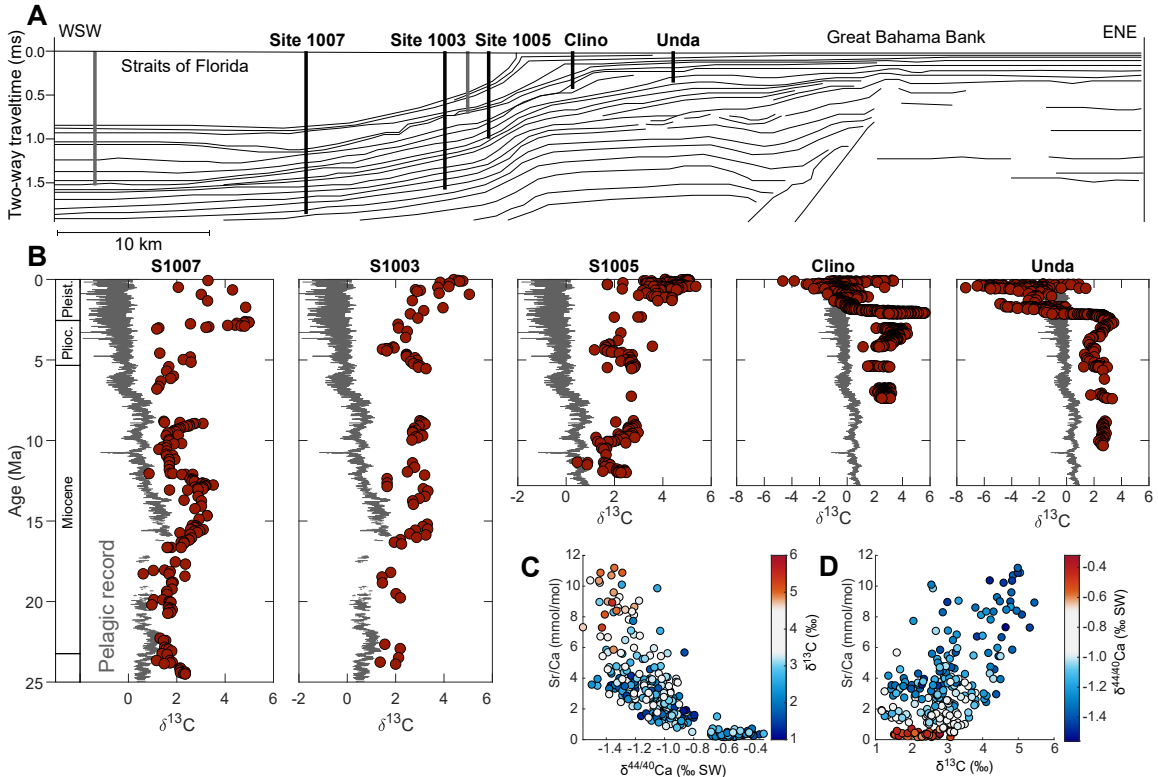


Figure 4: The variability in $\delta^{13}\text{C}_{\text{carb}}$ values from the Bahamas Transect (**A**), in cores taken across the bank-top and peri-platform slope, differ from the trends observed in deep-sea pelagic records (gray line, Westerhold et al. 2020). (**B**) Across the Bahamas transect (Eberli et al. 1997; Ginsburg 2001), the downcore trends are products of early marine diagenesis, meteoric alteration, and mixing between platform aragonite ($\delta^{13}\text{C} \sim 6\text{\textperthousand}$) and pelagic carbonate ($\delta^{13}\text{C} \sim 1\text{\textperthousand}$). Notably, in peri-platform cores (S1007, S1005, S1003) the increasing trends in $\delta^{13}\text{C}$ across the Plio-Pleistocene are also observed in platforms across the world (Swart 2008), and record mixing between platform aragonite, transported from the platform top, and both pelagic and/or diagenetic calcite and dolomite (Swart and Eberli 2005; Higgins et al. 2018). The cores from the bank top (Clino and Unda), record depleted $\delta^{13}\text{C}$ (down to $-7\text{\textperthousand}$), as a result of meteoric alteration during Plio-Pleistocene glacio-eustatic sea-level fall (Melim et al. 1995). (**C**) Downcore diagenetic recrystallization of aragonite can be tracked using $\delta^{44/40}\text{Ca}$ values (modern seawater as the reference standard) and Sr/Ca ratios. Primary platform aragonite sediments have low $\delta^{44/40}\text{Ca}$ and high Sr/Ca ratios (**D**, high $\delta^{13}\text{C}$), while diagenetic low-Mg calcite or dolomite have high $\delta^{44/40}\text{Ca}$ and low Sr/Ca ratios (Higgins et al. 2018).

401 top (Clino and Unda), adjacent slope (peri-platform), and the basinal environments in the deep
402 waters of the Straight of Florida (Fig. 4A, Eberli et al. 1997; Ginsburg 2001). Chemostratigraphies
403 measured from these cores provide important constraints on the geochemical signatures
404 of platform progradation, oscillating sea-level, and carbonate diagenesis.

405
406 Carbonate sediments from the Great Bahama Bank and peri-platform consists of a mixture
407 sourced from the bank top (platform aragonite) and open ocean (pelagic calcifiers) (Eberli et al.
408 1997; Ginsburg 2001). Stratigraphic variations in the proportion of platform and pelagic carbon-
409 ate have been linked to changes in eustatic sea-level, with pelagic carbonate dominating during
410 periods of low sea-level and platform-derived carbonate dominating during high sea-level (Swart
411 and Eberli 2005). During sea-level low stands, carbonate platform tops would be exposed, thus
412 shutting down aragonite production and export; conversely, during high stands, the platform is
413 flooded and a highly productive source of aragonite mud (Schlager et al. 1994). The significance
414 of sediment mixing, with respect to carbon isotope chemostratigraphy, is demonstrated by a
415 pronounced correlation between carbonate $\delta^{13}\text{C}$ values and the percentage of aragonite in cores
416 across the Bahamas transect (Swart and Eberli 2005). Aragonite mud, produced by calcareous
417 green algae such as *Halimeda* on the shallow platform top, has $\delta^{13}\text{C}$ values of $\sim +6\text{\textperthousand}$, while
418 pelagic calcite from coccolith and foraminifera tests have values $\sim +1\text{\textperthousand}$ (Lowenstam and Ep-
419 stein 1957; Swart and Eberli 2005). The elevated $\delta^{13}\text{C}$ values of platform aragonite mud are
420 a product of the larger fractionation factor for aragonite compared to calcite, in addition to
421 intense diurnal productivity which elevates the surface water $\delta^{13}\text{C}_{DIC}$ and carbonate satura-
422 tion in the day time when aragonite precipitates (Swart and Eberli 2005; Geyman and Maloof
423 2019). As a consequence, shedding of aragonite from the platform during high-stands (Schlager
424 et al. 1994) is recorded by a positive excursion in carbonate $\delta^{13}\text{C}$ values in peri-platform and
425 basinal sediments (Fig. 4). The influence of high-stand aragonite shedding on downslope $\delta^{13}\text{C}$
426 values is a global phenomenon, owing to the of high-amplitude glacioeustatic sea-level changes
427 in the Plio-Pleistocene (Fig. 4, Swart and Eberli 2005; Swart 2008). This positive ‘excursion’ is
428 an important example of carbonate $\delta^{13}\text{C}$ values not reflecting global DIC change, despite being
429 broadly correlative across the globe (Swart 2008).

430
431 Attributing excursions in $\delta^{13}\text{C}$ values to mixing of aragonite and pelagic calcite is complicated
432 by effects from early marine diagenesis. Geothermal temperature gradients drive the advection
433 of seawater into the platform interior from the slope (Kohout 1965; Henderson et al. 1999),
434 resulting in significant fluid-buffered diagensis of periplatform sediments (Melim et al. 2002;
435 Higgins et al. 2018). These advected fluids initially have $\delta^{13}\text{C}$ values that reflect the open
436 ocean ($\sim +1\text{\textperthousand}$). As a result, fluid-buffered diagenesis of platform derived aragonite results in
437 the resetting of carbon $\delta^{13}\text{C}$ values from $+5$ to $+1\text{\textperthousand}$ (Fig. 4D, Higgins et al. 2018; Ahm et
438 al. 2018). The process is recorded in the slope of the Great Bahamas Bank (Sites 1003 and
439 1007) as a down-core negative trend in $\delta^{13}\text{C}$ values, caused by the progressive dissolution of
440 metastable platform aragonite and re-precipitation of diagenetically-stable low magnesium cal-
441 crite or dolomite. Progressive aragonite replacement is also tracked by carbonate $\delta^{44/40}\text{Ca}$ values
442 and Sr/Ca ratios that correlate with carbonate $\delta^{13}\text{C}$ values in the upper ~ 150 m of the peri-
443 platform cores (Fig. 4C). Primary platform aragonite has low $\delta^{44/40}\text{Ca}$ values ($\sim -1.5\text{\textperthousand}$) and
444 high Sr/Ca ratios (~ 10 mmol/mol) due to the higher partition coefficients of Sr and ^{40}Ca for
445 aragonite than calcite (Tang et al. 2008). During aragonite replacement, $\delta^{44/40}\text{Ca}$ is reset to
446 higher values ($\sim -0.5\text{\textperthousand}$) and Sr/Ca ratios decrease (<1 mmol/mol, Higgins et al. 2018).

447
448 In addition to invigorating the advection of marine fluids into the platform interior, glacio-
449 eustatic sea-level changes in the Plio-Pleistocene resulted in extended periods of platform top
450 exposure (Vahrenkamp et al. 1991; Melim et al. 1995). During glacial maxima, platforms are
451 exposed and the freshwater aquifers within the exposed islands expand, causing meteoric dia-

genesis of previously deposited aragonite mud (Fig 4, core Clino and Unda). In the meteoric lens, groundwater acquires carbon from the degradation of organic matter in the surrounding sediment, which leads to the release of isotopically light CO₂ and the promotion of aragonite dissolution (Allan and Matthews 1977). Due to the influence of respired organic carbon in the freshwater lens, δ¹³C values of re-precipitated low magnesium calcite or dolomite can have very low values, consistent with observations from the Clino and Unda cores (Fig. 4B). During Pleistocene glacial-interglacial transitions, the Bahamas Bank has been exposed repeatedly, leading to a deep profile (+100 m) of meteoric diagenesis in platform top carbonates (Melim et al. 1995; Swart and Eberli 2005). With regard to carbon isotope chemostratigraphy, widespread synchronous negative excursions in carbonate δ¹³C values are expected as a result of sea-level fall and increase meteoric diagenesis of platform tops (provided significant organic carbon respiration occurs in the fresh water lens). These excursions can be useful stratigraphic markers for correlation, but the δ¹³C would not be tracking perturbations in the global carbon cycle (Allan and Matthews 1977; Dyer et al. 2015; Dyer et al. 2017). The most robust methods to fingerprint negative excursions as meteoric is by comparing other geochemical signatures (e.g., negative δ¹³C correlating with negative δ¹⁸O, or high Mn concentrations), in addition to petrographic observations of meteoric cements and sedimentological features such as exposure surfaces and root casts.

Owing to the extensive work on carbonate geochemistry from The Bahamas (e.g., Ginsburg 2001; Swart and Eberli 2005; Swart 2008; Oehlert et al. 2012; Oehlert and Swart 2014; Higgins et al. 2018), it is well established that Bahamian carbonate δ¹³C values do not reflect the δ¹³C_{DIC} of a well-mixed ocean in equilibrium with the atmosphere. While carbon isotope chemostratigraphy of pelagic deep-sea sediments may better reflect the global carbon cycle (e.g., Westerhold et al. 2020), the application of chemostratigraphy to ancient platform carbonates is not straight forward. Despite the many complications, in shallow-water pre-Mesozoic sediments across the world there are striking observations of large and broadly coeval stratigraphic excursions in carbonate δ¹³C values (for example: the Permian-Triassic boundary, the Ordovician-Silurian boundary, the Ediacaran Shuram excursion, snowball Earth cap carbonates). Below, we discuss the Neoproterozoic Era, a time period that shows both pronounced variability in δ¹³C_{carb} values (Fig. 5) and increasing geochronologic evidence for broadly synchronous perturbations (±5 Myr.) in shallow-water carbonate chemistry (Rooney et al. 2020; Swanson-Hysell et al. 2015).

4.2 The Neoproterozoic

Due to the lack of index fossils useful for biostratigraphy, carbon isotope chemostratigraphy has been applied widely to correlate Neoproterozoic carbonate successions (1000—541 Ma, Knoll et al. 1986; Kaufman et al. 1997; Halverson et al. 2005). The variability in δ¹³C values from Neoproterozoic carbonates dwarfs that of the Cenozoic deep sea record (population standard deviation = 4.7‰ vs. 0.6‰ respectively, Fig. 5). The Neoproterozoic record is characterized by high baseline values of +5—10‰ that are interrupted by dramatic negative excursions with values down to -15‰ (Fig. 5). The origin of the Neoproterozoic carbon isotope excursions is still widely debated, because δ¹³C values below -5‰ can not be explained by a traditional steady state carbon cycle model. Namely, in equation 6, inserting values for δ_{carb} that are below values of δ_{riv} will result in a negative number for the fraction of organic carbon buried. As a consequence, several studies have suggested alternative models for generating such negative δ¹³C values, including (1) short-term transient perturbations to the carbon cycle (e.g., Schrag et al. 2002; Rothman et al. 2003; Bjerrum and Canfield 2011), (2) carbonate diagenesis (Derry 2010; Knauth and Kennedy 2009) or (3) the formation of authigenic carbonate minerals (Tziperman et al. 2011; Schrag et al. 2013; Laakso and Schrag 2020). However, these models do not consider the possibility of broadly synchronous shifts in δ¹³C_{DIC} in platform waters (Swart 2008; Ahm

et al. 2019; Crockford et al. 2020), that may differ across individual basins on time-scales $>10^5$ years, and therefore are unrelated to changes in global DIC - analogous to observations from recent carbonate platforms.

The largest negative carbon isotope excursion in the Neoproterozoic is the Ediacaran Shuram-Wonoka excursion. This excursion is observed across the globe (e.g., Oman, Australia, Death Valley, Northwest Canada, Siberia) with minima $\delta^{13}\text{C}_{\text{carb}}$ values of $\sim-15\text{\textperthousand}$ (Fig. 5). Recent Re-Os ages confirm that the excursion is broadly synchronous, ranging between $\sim574\pm4.7$ to 567 ± 3.0 Ma (Rooney et al. 2020). These broad geochronological constraints, however, do not necessarily require that the excursion represent a global carbon cycle perturbation (*sensu* Fig. 2). Similarly to observations from recent platform carbonate, $\delta^{44/40}\text{Ca}$ data from the Wonoka Formation (South Australia) suggests that much of the carbonate that make up the anomaly was aragonite, originally formed in platformal settings, transported down slope, and recrystallized to low-Mg calcite during sediment-buffered diagenesis (Husson et al. 2015). Large systematic changes in $\delta^{44/40}\text{Ca}$ values (between -0.5 to $-2.0\text{\textperthousand}$) occur across the excursion (Fig. 5B,C), which is inconsistent with changes in the global calcium cycle and indicate that these sediments cannot represent the average carbonate burial sink (on timescale $>10^6$ yrs, Blättler and Higgins 2017). Moreover, in-situ measurements of $\delta^{13}\text{C}$ values via secondary ion mass spectrometry on individual carbonate grains, representing both authigenic phases and transported platform sediments, yielded a large range (from +5 to $-15\text{\textperthousand}$) from a single hand sample (Husson et al. 2020). These results suggest that the carbonates recording the Shuram excursion are recording a specific Ediacaran surface environment and not changes in the $\delta^{13}\text{C}_{\text{DIC}}$ of average seawater. The Shuram excursion may therefore be a broadly synchronous chemostratigraphic marker that track changes to global climate, tectonics, or sea-level over millions of years (Rooney et al. 2020), without tracking global $\delta^{13}\text{C}_{\text{DIC}}$.

Similar to the Shuram excursion, correlated changes in both carbonate $\delta^{13}\text{C}$ and $\delta^{44/40}\text{Ca}$ values are found in the globally distributed, basal Ediacaran carbonates (~635 Ma) that “cap” glacial deposits created during the pan-glacial “Snowball Earth” climate state (Hoffman et al. 2017). In these cap carbonates, $\delta^{13}\text{C}$ values in limestones reach $-6\text{\textperthousand}$, coinciding with low $\delta^{44/40}\text{Ca}$ values ($-2\text{\textperthousand}$) and high Sr/Ca ratios (~4 mmol/mol), consistent with signatures of sediment-buffered recrystallization of platform aragonite (Ahm et al. 2019). In contrast, dolostone portions of the cap sequence have higher $\delta^{13}\text{C}$ and $\delta^{44/40}\text{Ca}$ values, approaching values of modern seawater, suggesting that fluid-buffered dolomitization in reaction with Ediacaran seawater was responsible for resetting the primary low $\delta^{13}\text{C}$ values. These results indicate that the surface waters of platforms, where aragonite was forming, were significantly depleted in ^{13}C ($-6\text{\textperthousand}$), while the open ocean had $\delta^{13}\text{C}_{\text{DIC}}$ values close to 0\textperthousand . Multiple cap carbonate sections measured across individual basins reveal systematic spatial gradients in both $\delta^{13}\text{C}$ and $\delta^{44/40}\text{Ca}$ that are related to original basin geometry. The lowest values in both isotopic systems, representing sediment-buffered diagenesis, are found in sections from the platform interior, while the highest values, representing fluid-buffered diagenesis, are characteristic of the platform edge and upper slope (Ahm et al. 2019). These spatial trends are consistent with patterns of geothermal convection of fluids through recent platforms (Kohout 1965; Henderson et al. 1999), where warm, buoyantly riding fluid in the platform interior leads to compensatory flow of cold seawater into the sediment pile from the platform slope. An implication of these observations is that $\delta^{13}\text{C}$ values of dolostone, formed via fluid-buffered diagenesis with seawater, may be more reliable recorders of average seawater in comparison to shallow-water carbonate from the platform interior (Ahm et al. 2019; Hoffman and Lamothe 2019).

The results from the cap carbonates adds to the growing body of evidence that Neoproterozoic shallow water environments were characterized by large fluctuations in $\delta^{13}\text{C}$ values, decoupled

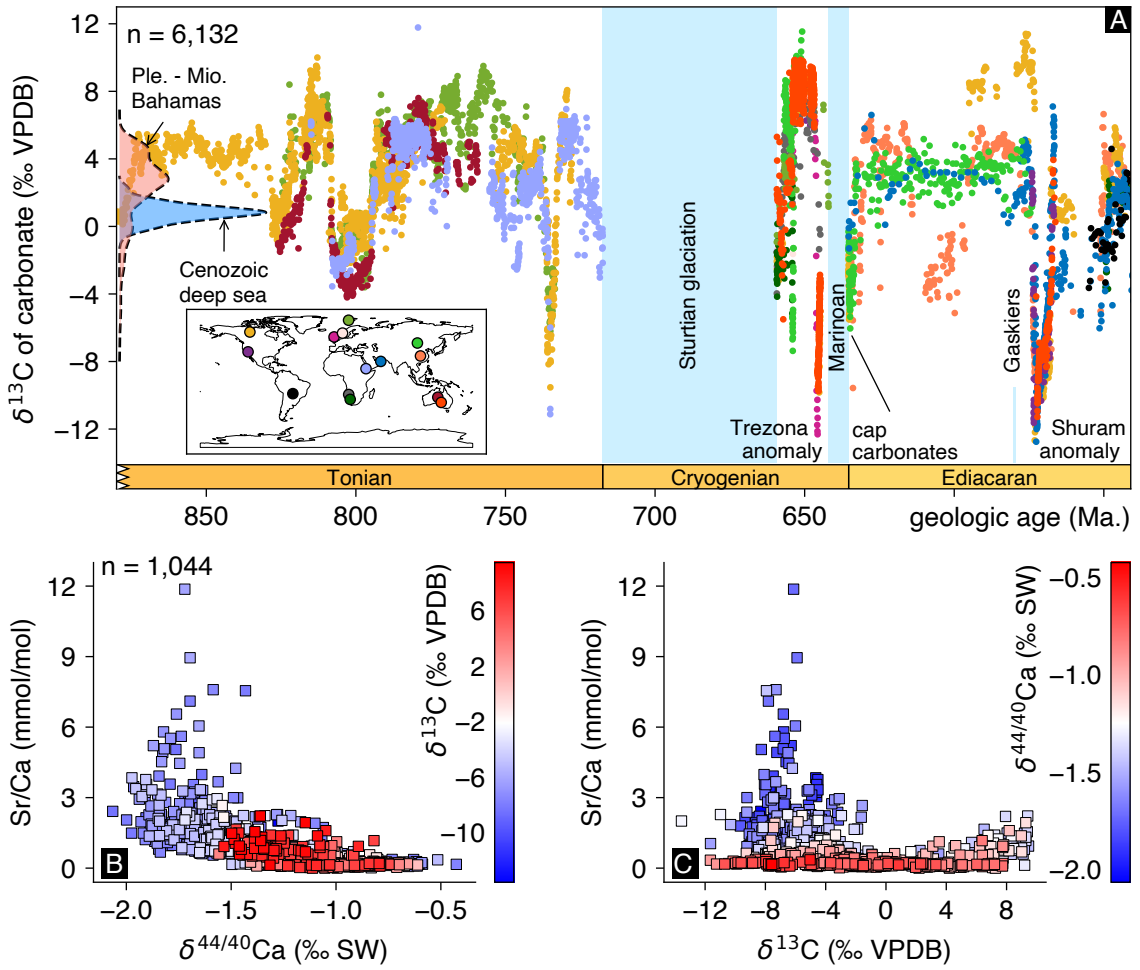


Figure 5: (A) A global compilation of $\delta^{13}\text{C}$ values from Neoproterozoic carbonates. The Tonian and Ediacaran age models are derived from Swanson-Hysell et al. (2015) and Rooney et al. (2020), with age constraints for the Cryogenian from Hoffman et al. (2017). Data points are color-coded to approximate geographic locality shown in the inset map. Kernel density estimates of distributions of $\delta^{13}\text{C}$ values from both the Bahamas (red, Pleistocene–Miocene in age; Swart and Eberli 2005; Melim et al. 1995) and deep sea sediment cores (blue, Cenozoic in age, Westerhold et al. 2020) are also shown. The height of each density estimate is arbitrary. (B,C) Cross-plots of $\delta^{44/40}\text{Ca}$, $\delta^{13}\text{C}$ and Sr/Ca values from carbonates with notable excursions in carbon isotopes: the Trezona and Shuram anomalies (Ahm et al. in review; Husson et al. 2015), and basal Ediacaran cap carbonates (Ahm et al. 2019).

from the average ocean value (Bold et al. 2020; Crockford et al. 2020). Various mechanisms have been proposed to explain the origin of very depleted $\delta^{13}\text{C}$ values in Neoproterozoic platform interior carbonates but, as of yet, no single hypothesis is accepted widely. Potentially important processes include nucleation kinetics associated with non-skeletal carbonate production (Hoffman and Lamothe 2019), the influence of microbial mats on the precipitation of carbonate, and the rapid invasion of CO_2 during periods of intense productivity (Lazar and Erez 1992). Whether or not these mechanisms could create broadly synchronous $\delta^{13}\text{C}$ excursions in shallow-water carbonates globally, and what boundary conditions are necessary for such synchronous changes, is an important avenue of ongoing research in Earth history.

562

563 **5 Future prospects**

564 The original framework of carbon isotope chemostratigraphy built on the assumption that
565 $\delta^{13}\text{C}_{\text{carb}}$ values directly record the $\delta^{13}\text{C}_{\text{DIC}}$ values of average seawater, in a well-mixed ocean
566 in equilibrium with the atmosphere (e.g., Broecker 1970; Kump and Arthur 1999). Research
567 though the last 20 years, however, has documented the importance of considering local vari-
568 ability in $\delta^{13}\text{C}_{\text{carb}}$ in platform environments (e.g., Holmden et al. 1998; Swart and Eberli 2005;
569 Oehlert and Swart 2014). These findings have demonstrated that carbon isotope chemostratig-
570 raphy from shallow-water strata rarely records changes in global $\delta^{13}\text{C}_{\text{DIC}}$ or the relative burial
571 flux of organic carbon, f_{org} .

572

573 It is likely that stratigraphic changes in $\delta^{13}\text{C}_{\text{carb}}$ broadly correlate both within basins and across
574 continents, driven by external forcings such as global climate change, tectonics, and sea-level.
575 To a first order, carbon isotope chemostratigraphy has provided robust correlation tie-points,
576 with uncertainties from hundred thousand to millions of years (Rooney et al. 2020; Swanson-
577 Hysell et al. 2015) – similarly to the time constraints provided by biostratigraphy applied in
578 shallow-water environments (Holland 2020). Importantly, these uncertainties should be consid-
579 ered when making arguments related to the global carbon cycle, which requires time constraints
580 on scales of $<10^5$ years in order to estimate average carbon burial fluxes.

581

582 Going forward, to help constrain globally-averaged carbonate burial on time-scales $>10^6$ years,
583 measurements of carbonate $\delta^{44/40}\text{Ca}$ values from thick carbonate successions can be a powerful
584 approach (Blättler and Higgins 2017; Higgins et al. 2018). Modeling studies of carbonate diage-
585 nesis that combine measurements of $\delta^{13}\text{C}$, $\delta^{44/40}\text{Ca}$, and Sr/Ca ratios, have demonstrated that
586 by embracing the diagenetic history of ancient carbonate it is possible to derived more accurate
587 records of seawater chemistry (Ahm et al. 2018). Specifically, carbonate successions that have
588 experienced early marine diagenesis and/or dolomitization may be important, and yet-to-be
589 explored, archives of ancient seawater chemistry (Ahm et al. 2019; Hoffman and Lamothe 2019;
590 Crockford et al. 2020). Finally, by accepting that shallow-water sedimentary records largely
591 reflect local carbon cycle dynamics, we may find that $\delta^{13}\text{C}$ measurements instead reflect the
592 local fingerprints of important climatic and evolutionary processes.

593

594 **6 Designated key papers**

595 The references below are a selected list (ordered by year of publication) of the ‘classics’ and
596 ‘best of the new’ that specifically evaluate the implications of diagenesis and local controls on
597 carbon isotope chemostratigraphy:

- 598 • Allan, J.R., Matthews, R.K., 1977. Carbon and oxygen isotopes as diagenetic and strati-
599 graphic tools: Surface and subsurface data, Barbados, West Indies. *Geology* 5 (1), 16–20.
600 *One of the first studies to show the impacts of diagenesis on carbon isotope chemostratig-
601 raphy*
- 602 • Banner, J.L., Hanson, G.N., 1990. Calculation of simultaneous isotopic and trace ele-
603 ment variations during water-rock interaction with applications to carbonate diagenesis.
604 *Geochimica et Cosmochimica Acta* 54 (11), 3123–3137. *Fundamental study that demon-
605 strates the sensitivity of carbonate $\delta^{13}\text{C}$ values to alteration using a fluid-rock interaction
606 model.*
- 607 • Patterson, W.P., Walter, L.M., 1994. Depletion of ^{13}C in seawater CO_2 on modern car-
608 bonate platforms: Significance for the carbon isotopic record of carbonates. *Geology* 22,
609 885–888. *One of the first studies to show significant isotopic variation of modern bank top
610 waters, due to the respiration of marine and terrestrial organic matter.*

- Holmden, C., Creaser, R.A., Muehlenbacks, K., Leslie, S.A., Bergström, S.M. et al. 1998. Isotopic evidence for geochemical decoupling between ancient epeiric seas and bordering oceans: Implications for secular curves. *Geology* 26 (6), 567–570. *One of the first studies to discuss the implications of local variations in geochemical aquafacies on secular carbon isotope trends in ancient platforms.*
- Swart, P.K., Eberli, G., 2005. The nature of the $\delta^{13}\text{C}$ of periplatform sediments: Implications for stratigraphy and the global carbon cycle. *Sedimentary Geology* 175 (1–4), 115–129. *Study that contextualizes the findings of the Bahamas drilling project and ODP Leg 166, and discuss the implications for carbon isotope chemostratigraphy.*
- Oehlert, A.M. Swart, P.K., 2014. Interpreting carbonate and organic carbon isotope covariance in the sedimentary record. *Nature Communications* 5 (1), 4672. *This study compares the variability of organic and carbonate $\delta^{13}\text{C}$ values from platform settings and find that covariation can result from mixing and sediment transport.*
- Higgins, J.A., Blättler, C.L., Lundstrom, E.A., Santiago-Ramos, D.P., Akhtar, A.A., Ahm, A-S.C., Bialik, O., Holmden, C., Bradbury, H., Murray, S.T., Swart. P.K., 2018. Mineralogy, early marine diagenesis, and the chemistry of shallow-water carbonate sediments. *Geochimica et Cosmochimica Acta* 220, 512–534. *This study demonstrates that early-marine diagenesis has large impact on geochemical records of $\delta^{44}\text{Ca}$ and $\delta^{13}\text{C}$ from platform settings.*
- Hoffman, P.F., and Lamothe, K.G., 2019. Seawater-buffered diagenesis, destruction of carbon isotope excursions, and the composition of DIC in Neoproterozoic oceans. *PNAS* 116 (38), 18874–18879. *This study finds that large spatial gradients in $\delta^{13}\text{C}$ exist across Neoproterozoic carbonate platforms as a result of early marine diagenesis.*
- Geyman, E.C., and Maloof, A.M., 2019. A diurnal carbon engine explains ^{13}C -enriched carbonates without increasing the global production of oxygen. *PNAS* 116 (49), 24433–24439. *This study demonstrates that highly ^{13}C -enriched carbonate can be produced in platform environments without increasing the local or global burial flux of organic carbon.*

References

- Ahm, Anne-Sofie C, Bjerrum, Christian J, Blättler, Clara L, Swart, Peter K, and Higgins, John A (2018). “Quantifying early marine diagenesis in shallow-water carbonate sediments”. In: *Geochimica et Cosmochimica Acta* 236, pp. 140–159. DOI: [10.1016/j.gca.2018.02.042](https://doi.org/10.1016/j.gca.2018.02.042).
- Ahm, Anne-Sofie C, Maloof, Adam C, Macdonald, Francis A, Hoffman, Paul F, Bjerrum, Christian J, Bold, Uyanga, Rose, Catherine V, Strauss, Justin V, and Higgins, John A (2019). “An early diagenetic deglacial origin for basal Ediacaran “cap dolostones””. In: *Earth and Planetary Science Letters* 506, pp. 292–307. DOI: [10.1016/j.epsl.2018.10.046](https://doi.org/10.1016/j.epsl.2018.10.046).
- Allan, JR and Matthews, RK (1977). “Carbon and oxygen isotopes as diagenetic and stratigraphic tools: surface and subsurface data, Barbados, West Indies”. In: *Geology* 5.1, pp. 16–20. DOI: [10.1130/0091-7613\(1977\)5<16:CAOIAD>2.0.CO;2](https://doi.org/10.1130/0091-7613(1977)5<16:CAOIAD>2.0.CO;2).
- Banner, Jay L and Hanson, Gilbert N (1990). “Calculation of simultaneous isotopic and trace element variations during water-rock interaction with applications to carbonate diagenesis”. In: *Geochimica et Cosmochimica Acta* 54.11, pp. 3123–3137.
- Beeler, Scott R., Gomez, Fernando J., and Bradley, Alexander S. (2020). “Controls of extreme isotopic enrichment in modern microbialites and associated abiogenic carbonates”. In: *Geochimica et Cosmochimica Acta* 269, pp. 136–149. DOI: [10.1016/j.gca.2019.10.022](https://doi.org/10.1016/j.gca.2019.10.022).
- Berner, Robert A (2006). “GEOCARBSULF: a combined model for Phanerozoic atmospheric O_2 and CO_2 ”. In: *Geochimica et Cosmochimica Acta* 70.23, pp. 5653–5664. DOI: [10.1016/j.gca.2005.11.032](https://doi.org/10.1016/j.gca.2005.11.032).

- 658 Birgel, D., Meister, P., Lundberg, R., Horath, T. D., Bontognali, T. R. R., Bahniuk, A. M.,
659 Rezende, C. E. de, Vasconcelos, C., and McKenzie, J. A. (2015). "Methanogenesis produces
660 strong $\delta^{13}\text{C}$ enrichment in stromatolites of Lagoa Salgada, Brazil: a modern analogue for
661 Palaeo-/Neoproterozoic stromatolites?" In: *Geobiology* 13.3, pp. 245–266. DOI: [10.1111/gbi.12130](https://doi.org/10.1111/gbi.12130).
- 663 Bjerrum, Christian J and Canfield, Donald E (2004). "New insights into the burial history of
664 organic carbon on the early Earth". In: *Geochemistry, Geophysics, Geosystems* 5.8.
665 – (2011). "Towards a quantitative understanding of the late Neoproterozoic carbon cycle". In:
666 *Proceedings of the National Academy of Sciences* 108.14, p. 5542. DOI: [10.1073/pnas.1101755108](https://doi.org/10.1073/pnas.1101755108).
- 668 Blättler, Clara L and Higgins, John A (2017). "Testing Urey's carbonate–silicate cycle using the
669 calcium isotopic composition of sedimentary carbonates". In: *Earth and Planetary Science
670 Letters* 479, pp. 241–251. DOI: [10.1016/j.epsl.2017.09.033](https://doi.org/10.1016/j.epsl.2017.09.033).
- 671 Bold, Uyanga, Ahm, Anne-Sofie C, Schrag, Daniel P, Higgins, John A, Jamsran, Erdenebayar,
672 and Macdonald, Francis A (2020). "Effect of dolomitization on isotopic records from Neo-
673 proterozoic carbonates in southwestern Mongolia". In: *Precambrian Research* 350, p. 105902.
674 DOI: [10.1016/j.precamres.2020.105902](https://doi.org/10.1016/j.precamres.2020.105902).
- 675 Bown, Paul R., Lees, Jackie A., and Young, Jeremy R. (2004). "Calcareous nannoplankton
676 evolution and diversity through time". In: ed. by Hans R. Thierstein and Jeremy R. Young.
677 Berlin, Heidelberg: Springer Berlin Heidelberg, pp. 481–508. DOI: [10.1007/978-3-662-06278-4_18](https://doi.org/10.1007/978-3-662-06278-4_18).
- 679 Broecker, Wallace S (1970). "A boundary condition on the evolution of atmospheric oxygen".
680 In: *Journal of Geophysical Research* 75.18, pp. 3553–3557. DOI: [10.1029/JC075i018p03553](https://doi.org/10.1029/JC075i018p03553).
- 681 Campeau, Audrey, Wallin, Marcus B, Giesler, Reiner, Löfgren, Stefan, Mört, Carl-Magnus,
682 Schiff, Sherry, Venkiteswaran, Jason J, and Bishop, Kevin (2017). "Multiple sources and
683 sinks of dissolved inorganic carbon across Swedish streams, refocusing the lens of stable C
684 isotopes". In: *Scientific Reports* 7.1, pp. 1–14. DOI: [10.1038/s41598-017-09049-9](https://doi.org/10.1038/s41598-017-09049-9).
- 685 Canfield, Donald E., Knoll, Andrew H., Poulton, Simon W., Narbonne, Guy M., and Dunning,
686 Gregory R. (2020). "Carbon isotopes in clastic rocks and the Neoproterozoic carbon cycle".
687 In: *American Journal of Science* 320.2, pp. 97–124. DOI: [10.2475/02.2020.01](https://doi.org/10.2475/02.2020.01).
- 688 Clark, Ian D., Fontes, Jean-Charles, and Fritz, Peter (1992). "Stable isotope disequilibria in
689 travertine from high pH waters: Laboratory investigations and field observations from Oman".
690 In: *Geochimica et Cosmochimica Acta* 56.5, pp. 2041–2050. DOI: [10.1016/0016-7037\(92\)90328-G](https://doi.org/10.1016/0016-7037(92)90328-G).
- 692 Claypool, George E. and Kaplan, I. R. (1974). "The Origin and Distribution of Methane in
693 Marine Sediments". In: *Natural Gases in Marine Sediments*. Ed. by Isaac R. Kaplan. Springer
694 US, pp. 99–139. DOI: [10.1007/978-1-4684-2757-8_8](https://doi.org/10.1007/978-1-4684-2757-8_8).
- 695 Craig, Harmon (1953). "The geochemistry of the stable carbon isotopes". In: *Geochimica et
696 Cosmochimica Acta* 3.2-3, pp. 53–92. DOI: [10.1016/0016-7037\(53\)90001-5](https://doi.org/10.1016/0016-7037(53)90001-5).
- 697 Crockford, Peter W, Kunzmann, Marcus, Blättler, Clara L, Kalderon-Asael, Boriana, Mur-
698 phy, Jack G, Ahm, Anne-Sofie C, Sharoni, Shlomit, Halverson, Galen P, Planavsky, Noah J,
699 Halevy, Itay, and Higgins, John A (2020). "Reconstructing Neoproterozoic seawater chemistry
700 from early diagenetic dolomite". In: *Geology*. DOI: [10.1130/G48213.1](https://doi.org/10.1130/G48213.1).
- 701 Derry, Louis A (2010). "A burial diagenesis origin for the Ediacaran Shuram–Wonoka carbon
702 isotope anomaly". In: *Earth and Planetary Science Letters* 294.1-2, pp. 152–162. DOI: [10.1016/j.epsl.2010.03.022](https://doi.org/10.1016/j.epsl.2010.03.022).
- 704 Dyer, Blake, Higgins, John A, and Maloof, Adam C (2017). "A probabilistic analysis of mete-
705 orically altered $\delta^{13}\text{C}$ chemostratigraphy from late Paleozoic ice age carbonate platforms". In:
706 *Geology* 45.2, pp. 135–138. DOI: [10.1130/G38513.1](https://doi.org/10.1130/G38513.1).

- 707 Dyer, Blake, Maloof, Adam C, and Higgins, John A (2015). "Glacioeustasy, meteoric diagenesis, and the carbon cycle during the Middle Carboniferous". In: *Geochemistry, Geophysics, Geosystems* 16.10, pp. 3383–3399. DOI: [10.1002/2015GC006002](https://doi.org/10.1002/2015GC006002).
- 708 Eberli, Gregor P, Swart, PK, McNeill, DF, Kenter, JAM, Anselmetti, FS, Melim, LA, and
709 Ginsburg, RN (1997). "A synopsis of the Bahamas Drilling Project: results from two deep
710 core borings drilled on the Great Bahama Bank". In: *Proceedings of the ocean drilling program, initial reports*. Vol. 166, pp. 23–41. DOI: [10.2973/odp.proc.ir.166.1997](https://doi.org/10.2973/odp.proc.ir.166.1997).
- 711 Fantle, M. S., Maher, K. M., and DePaolo, D. J. (2010). "Isotopic approaches for quantifying
712 the rates of marine burial diagenesis". In: *Reviews of Geophysics* 48.3. DOI: <https://doi.org/10.1029/2009RG000306>.
- 713 Fantle, Matthew S. and DePaolo, Donald J. (2007). "Ca isotopes in carbonate sediment and
714 pore fluid from ODP Site 807A: The Ca^{2+} (aq)-calcite equilibrium fractionation factor and
715 calcite recrystallization rates in Pleistocene sediments". In: *Geochimica et Cosmochimica Acta*
716 71.10, pp. 2524–2546. DOI: [10.1016/j.gca.2007.03.006](https://doi.org/10.1016/j.gca.2007.03.006).
- 717 Fantle, Matthew S. and Higgins, John (2014). "The effects of diagenesis and dolomitization on
718 Ca and Mg isotopes in marine platform carbonates: Implications for the geochemical cycles
719 of Ca and Mg". In: *Geochimica et Cosmochimica Acta* 142, pp. 458–481. DOI: [10.1016/j.gca.2014.07.025](https://doi.org/10.1016/j.gca.2014.07.025).
- 720 Geyman, Emily C and Maloof, Adam C (2019). "A diurnal carbon engine explains ^{13}C -enriched
721 carbonates without increasing the global production of oxygen". In: *Proceedings of the National
722 Academy of Sciences* 116.49, pp. 24433–24439. DOI: [10.1073/pnas.1908783116](https://doi.org/10.1073/pnas.1908783116).
- 723 Ginsburg, Robert N (2001). "The Bahamas drilling project: background and acquisition of cores
724 and logs". In: DOI: [10.2110/pec.01.70.0003](https://doi.org/10.2110/pec.01.70.0003).
- 725 Gregor, B (1970). "Denudation of the continents". In: *Nature* 228.5268, pp. 273–275. DOI: [10.1038/228273a0](https://doi.org/10.1038/228273a0).
- 726 Gussone, Nikolaus, Ahm, Anne-Sofie C, Lau, Kimberly V, and Bradbury, Harold J (2020).
727 "Calcium isotopes in deep time: Potential and limitations". In: *Chemical Geology*, p. 119601.
- 728 Gussone, Nikolaus, Böhm, Florian, Eisenhauer, Anton, Dietzel, Martin, Heuser, Alexander,
729 Teichert, Barbara M. A., Reitner, Joachim, Wörheide, Gert, and Dullo, Wolf-Christian (2005).
730 "Calcium isotope fractionation in calcite and aragonite". In: *Geochimica et Cosmochimica Acta*
731 69.18, pp. 4485–4494. DOI: [10.1016/j.gca.2005.06.003](https://doi.org/10.1016/j.gca.2005.06.003).
- 732 Halverson, Galen P, Hoffman, Paul F, Schrag, Daniel P, Maloof, Adam C, and Rice, A Hugh N
733 (2005). "Toward a Neoproterozoic composite carbon-isotope record". In: *GSA bulletin* 117.9-
734 10, pp. 1181–1207. DOI: [10.1130/B25630.1](https://doi.org/10.1130/B25630.1).
- 735 Harper, Brandon B., Puga-Bernabéu, Ángel, Droxler, André W, Webster, Jody M., Gischler,
736 Eberhard, Tiwari, Manish, Lado-Insua, Tania, Thomas, Alex L., Morgan, Sally, Jovane, Luigi,
737 and Röhl, Ursula (2015). "Mixed Carbonate–Siliciclastic Sedimentation Along the Great Barrier
738 Reef Upper Slope: A Challenge To the Reciprocal Sedimentation Model". In: *Journal of
739 Sedimentary Research* 85.9, pp. 1019–1036. DOI: [10.2110/jsr.2015.58.1](https://doi.org/10.2110/jsr.2015.58.1).
- 740 Hayes, John M., Strauss, Harald, and Kaufman, Alan J. (1999). "The abundance of ^{13}C in
741 marine organic matter and isotopic fractionation in the global biogeochemical cycle of carbon
742 during the past 800 Ma". In: *Chemical Geology* 161.1, pp. 103–125. DOI: [10.1016/S0009-2541\(99\)00083-2](https://doi.org/10.1016/S0009-2541(99)00083-2).
- 743 Henderson, Gideon M, Slowey, Niall C, and Haddad, Geoff A (1999). "Fluid flow through
744 carbonate platforms: Constraints from $^{234}\text{U}/^{238}\text{U}$ and Cl^- in Bahamas pore-waters". In: *Earth
745 and Planetary Science Letters* 169.1-2, pp. 99–111. DOI: [10.1016/S0012-821X\(99\)00065-5](https://doi.org/10.1016/S0012-821X(99)00065-5).
- 746 Higgins, J.A., Fischer, W.W., and Schrag, D.P. (2009). "Oxygenation of the ocean and sediments:
747 Consequences for the seafloor carbonate factory". In: *Earth and Planetary Science Letters*
748 284.1-2, pp. 25–33. DOI: [10.1016/j.epsl.2009.03.039](https://doi.org/10.1016/j.epsl.2009.03.039).
- 749 Higgins, John A, Blättler, Clara L, Lundstrom, EA, Santiago-Ramos, DP, Akhtar, AA, Ahm,
750 Anne-Sofie C, Bialik, O, Holmden, Chris, Bradbury, H, Murray, ST, et al. (2018). "Mineral-

- ogy, early marine diagenesis, and the chemistry of shallow-water carbonate sediments". In: *Geochimica et Cosmochimica Acta* 220, pp. 512–534. DOI: [10.1016/j.gca.2017.09.046](https://doi.org/10.1016/j.gca.2017.09.046).
- Hoffman, Paul F, Abbot, Dorian S, Ashkenazy, Yosef, Benn, Douglas I, Brocks, Jochen J, Cohen, Phoebe A, Cox, Grant M, Creveling, Jessica R, Donnadieu, Yannick, Erwin, Douglas H, et al. (2017). "Snowball Earth climate dynamics and Cryogenian geology-geobiology". In: *Science Advances* 3.11, e1600983. DOI: [10.1126/sciadv.1600983](https://doi.org/10.1126/sciadv.1600983).
- Hoffman, Paul F and Lamothe, Kelsey G (2019). "Seawater-buffered diagenesis, destruction of carbon isotope excursions, and the composition of DIC in Neoproterozoic oceans". In: *Proceedings of the National Academy of Sciences* 116, pp. 18874–18879. DOI: [10.1073/pnas.1909570116](https://doi.org/10.1073/pnas.1909570116).
- Holland, Steven M. (2020). "The Stratigraphy of Mass Extinctions and Recoveries". In: *Annual Review of Earth and Planetary Sciences* 48.1, pp. 75–97. DOI: [10.1146/annurev-earth-071719-054827](https://doi.org/10.1146/annurev-earth-071719-054827).
- Holmden, C., Panchuk, K., and Finney, S.C. (2012). "Tightly coupled records of Ca and C isotope changes during the Hirnantian glaciation event in an epeiric sea setting". In: *Geochimica et Cosmochimica Acta* 98, pp. 94–106. DOI: [10.1016/j.gca.2012.09.017](https://doi.org/10.1016/j.gca.2012.09.017).
- Holmden, Chris, Creaser, RA, Muehlenbachs, KLSA, Leslie, SA, and Bergstrom, SM (1998). "Isotopic evidence for geochemical decoupling between ancient epeiric seas and bordering oceans: implications for secular curves". In: *Geology* 26.6, pp. 567–570. DOI: [10.1130/0091-7613\(1998\)026<0567:IEFGDB>2.3.CO;2](https://doi.org/10.1130/0091-7613(1998)026<0567:IEFGDB>2.3.CO;2).
- Hovland, Martin, Talbot, Michael R., Qvale, Henning, Olaussen, Snorre, and Aasberg, Lars (1987). "Methane-related carbonate cements in pockmarks of the North Sea". In: *Journal of Sedimentary Research* 57.5, pp. 881–892. DOI: [10.1306/212F8C92-2B24-11D7-8648000102C1865D](https://doi.org/10.1306/212F8C92-2B24-11D7-8648000102C1865D).
- Husson, Jon M, Higgins, John A, Maloof, Adam C, and Schoene, Blair (2015). "Ca and Mg isotope constraints on the origin of Earth's deepest $\delta^{13}\text{C}$ excursion". In: *Geochimica et Cosmochimica Acta* 160, pp. 243–266. DOI: [10.1016/j.gca.2015.03.012](https://doi.org/10.1016/j.gca.2015.03.012).
- Husson, Jon M, Linzmeier, Benjamin J, Kitajima, Kouki, Ishida, Akizumi, Maloof, Adam C, Schoene, Blair, Peters, Shanan E, and Valley, John W (2020). "Large isotopic variability at the micron-scale in 'Shuram' excursion carbonates from South Australia". In: *Earth and Planetary Science Letters* 538, p. 116211. DOI: [10.1016/j.epsl.2020.116211](https://doi.org/10.1016/j.epsl.2020.116211).
- Jacobson, Andrew D. and Holmden, Chris (2008). " $\delta^{44}\text{Ca}$ evolution in a carbonate aquifer and its bearing on the equilibrium isotope fractionation factor for calcite". In: *Earth and Planetary Science Letters* 270.3, pp. 349–353. DOI: [10.1016/j.epsl.2008.03.039](https://doi.org/10.1016/j.epsl.2008.03.039).
- Kaufman, A. J., Knoll, A. H., and Narbonne, G. M. (1997). "Isotopes, ice ages, and terminal Proterozoic earth history". In: *Proceedings of the National Academy of Sciences* 94.13, pp. 6600–6605. DOI: [10.1073/pnas.94.13.6600](https://doi.org/10.1073/pnas.94.13.6600).
- Keigwin, LD and Shackleton, NJ (1980). "Uppermost Miocene carbon isotope stratigraphy of a piston core in the equatorial Pacific". In: *Nature* 284.5757, pp. 613–614. DOI: [10.1038/284613a0](https://doi.org/10.1038/284613a0).
- Keith, ML and Weber, JN (1964). "Carbon and oxygen isotopic composition of selected limestones and fossils". In: *Geochimica et cosmochimica acta* 28.10-11, pp. 1787–1816. DOI: [10.1016/0016-7037\(64\)90022-5](https://doi.org/10.1016/0016-7037(64)90022-5).
- Khadka, Mitra B., Martin, Jonathan B., and Jin, Jin (2014). "Transport of dissolved carbon and CO₂ degassing from a river system in a mixed silicate and carbonate catchment". In: *Journal of Hydrology* 513, pp. 391–402. DOI: [10.1016/j.jhydrol.2014.03.070](https://doi.org/10.1016/j.jhydrol.2014.03.070).
- King, Arthur S and Birge, Raymond T (1929). "An isotope of carbon, mass 13". In: *Nature* 124.3117, pp. 127–127.
- Knauth, L. Paul and Kennedy, Martin J. (2009). "The late Precambrian greening of the Earth". In: *Nature* 460.7256, pp. 728–732. DOI: [10.1038/nature08213](https://doi.org/10.1038/nature08213).

- 808 Knoll, A.H., Hayes, J.M., Kaufman, A.J., Swett, K., and Lambert, I.B. (1986). "Secular variation
809 in carbon isotope ratios from Upper Proterozoic successions of Svalbard and East Greenland".
810 In: *Nature* 321.6073, pp. 832–838. DOI: [10.1038/321832a0](https://doi.org/10.1038/321832a0).
- 811 Kohout, F.A. (1965). "A hypothesis concerning cyclic flow of salt water related to geothermal
812 heating in the Floridan aquifer". In: *New York Academy of Sciences Transactions* 28, pp. 249–
813 271. DOI: [10.1111/j.2164-0947.1965.tb02879.x](https://doi.org/10.1111/j.2164-0947.1965.tb02879.x).
- 814 Komar, N. and Zeebe, R. E. (2016). "Calcium and calcium isotope changes during carbon cycle
815 perturbations at the end-Permian: END-PERMIAN CALCIUM CYCLE". In: *Paleoceanography* 31.1, pp. 115–130. DOI: [10.1002/2015PA002834](https://doi.org/10.1002/2015PA002834).
- 817 Kump, L. R, Arthur, M. A, Patzkowsky, M. E, Gibbs, M. T, Pinkus, D. S, and Sheehan, P. M
818 (1999). "A weathering hypothesis for glaciation at high atmospheric pCO₂ during the Late
819 Ordovician". In: *Palaeogeography, Palaeoclimatology, Palaeoecology* 152.1, pp. 173–187. DOI:
820 [10.1016/S0031-0182\(99\)00046-2](https://doi.org/10.1016/S0031-0182(99)00046-2).
- 821 Kump, Lee R and Arthur, Michael A (1999). "Interpreting carbon-isotope excursions: carbonates
822 and organic matter". In: *Chemical Geology* 161.1-3, pp. 181–198. DOI: [10.1016/S0009-2541\(99\)00086-8](https://doi.org/10.1016/S0009-2541(99)00086-8).
- 824 Laakso, Thomas A and Schrag, Daniel P (2020). "The role of authigenic carbonate in Neoproterozoic
825 carbon isotope excursions". In: *Earth and Planetary Science Letters* 549, p. 116534.
826 DOI: [10.1016/j.epsl.2020.116534](https://doi.org/10.1016/j.epsl.2020.116534).
- 827 Lazar, Boaz and Erez, Jonathan (1992). "Carbon geochemistry of marine-derived brines: I.
828 δ¹³C depletions due to intense photosynthesis". In: *Geochimica et Cosmochimica Acta* 56.1,
829 pp. 335–345. DOI: [10.1016/0016-7037\(92\)90137-8](https://doi.org/10.1016/0016-7037(92)90137-8).
- 830 Loutit, Tom S and Kennett, James P (1979). "Application of carbon isotope stratigraphy to
831 late Miocene shallow marine sediments, New Zealand". In: *Science* 204.4398, pp. 1196–1199.
832 DOI: [10.1126/science.204.4398.1196](https://doi.org/10.1126/science.204.4398.1196).
- 833 Lowenstam, Heinz A and Epstein, Samuel (1957). "On the origin of sedimentary aragonite
834 needles of the Great Bahama Bank". In: *The Journal of Geology* 65.4, pp. 364–375. DOI:
835 [10.1086/626439](https://doi.org/10.1086/626439).
- 836 Lynch-Stieglitz, Jean, Stocker, Thomas F, Broecker, Wallace S, and Fairbanks, Richard G
837 (1995). "The influence of air-sea exchange on the isotopic composition of oceanic carbon:
838 Observations and modeling". In: *Global Biogeochemical Cycles* 9.4, pp. 653–665. DOI: [10.1029/95GB02574](https://doi.org/10.1029/95GB02574).
- 840 Maher, D. T., Santos, I. R., Golsby-Smith, L., Gleeson, J., and Eyre, B. D. (2013). "Groundwater-
841 derived dissolved inorganic and organic carbon exports from a mangrove tidal creek: The
842 missing mangrove carbon sink?" In: *Limnology and Oceanography* 58.2, pp. 475–488. DOI:
843 [10.4319/lo.2013.58.2.0475](https://doi.org/10.4319/lo.2013.58.2.0475).
- 844 Melim, L. A, Westphal, H, Swart, P. K, Eberli, G. P, and Munnecke, A (2002). "Questioning
845 carbonate diagenetic paradigms: evidence from the Neogene of the Bahamas". In: *Marine
846 Geology* 185.1, pp. 27–53. DOI: [10.1016/S0025-3227\(01\)00289-4](https://doi.org/10.1016/S0025-3227(01)00289-4).
- 847 Melim, Leslie A, Swart, Peter K, and Maliva, Robert G (1995). "Meteoric-like fabrics forming in
848 marine waters: Implications for the use of petrography to identify diagenetic environments".
849 In: *Geology*, p. 4. DOI: [10.1130/0091-7613\(1995\)023<0755:MLFFIM>2.3.CO;2](https://doi.org/10.1130/0091-7613(1995)023<0755:MLFFIM>2.3.CO;2).
- 850 Murray, Sean T., Higgins, John A., Holmden, Chris, Lu, Chaojin, and Swart, Peter K. (2021).
851 "Geochemical fingerprints of dolomitization in Bahamian carbonates: Evidence from sulphur,
852 calcium, magnesium and clumped isotopes". In: *Sedimentology* 68.1, pp. 1–29. DOI: doi.org/10.1111/sed.12775.
- 854 Nier, Alfred O and Gulbransen, Earl A (1939). "Variations in the relative abundance of the
855 carbon isotopes". In: *Journal of the American Chemical Society* 61.3, pp. 697–698. DOI: doi.org/10.1021/ja01872a047.
- 857 Oehlert, Amanda M, Lamb-Wozniak, Kathryn A, Devlin, Quinn B, Mackenzie, Greta J, Reijmer,
858 John JG, and Swart, Peter K (2012). "The stable carbon isotopic composition of organic

- material in platform derived sediments: implications for reconstructing the global carbon cycle". In: *Sedimentology* 59.1, pp. 319–335. DOI: [10.1111/j.1365-3091.2011.01273.x](https://doi.org/10.1111/j.1365-3091.2011.01273.x).
- Oehlert, Amanda M and Swart, Peter K (2014). "Interpreting carbonate and organic carbon isotope covariance in the sedimentary record". In: *Nature Communications* 5.1, pp. 1–7. DOI: [10.1038/ncomms5672](https://doi.org/10.1038/ncomms5672).
- Opdyke, Bradley N. and Wilkinson, Bruce H. (1988). "Surface area control of shallow cratonic to deep marine carbonate accumulation". In: *Paleoceanography* 3.6, pp. 685–703. DOI: doi.org/10.1029/PA003i006p00685.
- Patterson, William P and Walter, Lynn M (1994). "Depletion of ^{13}C in seawater ΣCO_2 on modern carbonate platforms: Significance for the carbon isotopic record of carbonates". In: *Geology* 22.10, pp. 885–888. DOI: [10.1130/0091-7613\(1994\)022<0885:DOCISC>2.3.CO;2](https://doi.org/10.1130/0091-7613(1994)022<0885:DOCISC>2.3.CO;2).
- Pearson, A (2010). "Pathways of carbon assimilation and their impact on organic matter values $\delta^{13}\text{C}$ ". In: *Handbook of Hydrocarbon and Lipid Microbiology*. DOI: [10.1007/978-3-540-77587-4_9](https://doi.org/10.1007/978-3-540-77587-4_9).
- Popp, Brian N, Laws, Edward A, Bidigare, Robert R, Dore, John E, Hanson, Kristi L, and Wakeham, Stuart G (1998). "Effect of phytoplankton cell geometry on carbon isotopic fractionation". In: *Geochimica et cosmochimica acta* 62.1, pp. 69–77. DOI: [10.1016/S0016-7037\(97\)00333-5](https://doi.org/10.1016/S0016-7037(97)00333-5).
- Richardson, Christina M., Dulai, Henrietta, Popp, Brian N., Ruttenberg, Kathleen, and Fackrell, Joseph K. (2017). "Submarine groundwater discharge drives biogeochemistry in two Hawaiian reefs". In: *Limnology and Oceanography* 62.S1, S348–S363. DOI: doi.org/10.1002/lno.10654.
- Rodriguez Blanco, Leticia, Eberli, Gregor P., Weger, Ralf J., Swart, Peter K., Tenaglia, Maximilian, Rueda Sanchez, Laura E., and McNeill, Donald F. (2020). "Periplatform ooze in a mixed siliciclastic-carbonate system - Vaca Muerta Formation, Argentina". In: *Sedimentary Geology* 396, p. 105521. DOI: [10.1016/j.sedgeo.2019.105521](https://doi.org/10.1016/j.sedgeo.2019.105521).
- Romanek, Christopher S, Grossman, Ethan L, and Morse, John W (1992). "Carbon isotopic fractionation in synthetic aragonite and calcite: effects of temperature and precipitation rate". In: *Geochimica et cosmochimica acta* 56.1, pp. 419–430. DOI: [10.1016/0016-7037\(92\)90142-6](https://doi.org/10.1016/0016-7037(92)90142-6).
- Ronov, AB, Khain, VE, Balukhovsky, AN, and Seslavinsky, KB (1980). "Quantitative analysis of Phanerozoic sedimentation". In: *Sedimentary Geology* 25.4, pp. 311–325. DOI: [10.1016/0037-0738\(80\)90067-6](https://doi.org/10.1016/0037-0738(80)90067-6).
- Rooney, Alan D, Cantine, Marjorie D, Bergmann, Kristin D, Gómez-Pérez, Irene, Al Baloushi, Badar, Boag, Thomas H, Busch, James F, Sperling, Erik A, and Strauss, Justin V (2020). "Calibrating the coevolution of Ediacaran life and environment". In: *Proceedings of the National Academy of Sciences* 117.29, pp. 16824–16830. DOI: [10.1073/pnas.2002918117](https://doi.org/10.1073/pnas.2002918117).
- Rothman, D.H., Hayes, J.M., and Summons, R.E. (2003). "Dynamics of the Neoproterozoic carbon cycle". In: *Proceedings of the National Academy of Sciences* 100.14, pp. 8124–8129. DOI: [10.1073/pnas.0832439100](https://doi.org/10.1073/pnas.0832439100).
- Saltzman, Matthew R (2005). "Phosphorus, nitrogen, and the redox evolution of the Paleozoic oceans". In: *Geology* 33.7, pp. 573–576. DOI: [10.1130/G21535.1](https://doi.org/10.1130/G21535.1).
- Schidlowski, Manfred, Eichmann, Rudolf, and Junge, Christian E (1975). "Precambrian sedimentary carbonates: carbon and oxygen isotope geochemistry and implications for the terrestrial oxygen budget". In: *Precambrian Research* 2.1, pp. 1–69. DOI: [10.1016/0301-9268\(75\)90018-2](https://doi.org/10.1016/0301-9268(75)90018-2).
- Schlager, Wolfgang, Reijmer, John JG, and Droxler, AW (1994). "Highstand shedding of carbonate platforms". In: *Journal of Sedimentary Research* 64.3b, pp. 270–281. DOI: [10.1306/D4267FAA-2B26-11D7-8648000102C1865D](https://doi.org/10.1306/D4267FAA-2B26-11D7-8648000102C1865D).

- 908 Schoene, Blair (2014). "4.10 - U-Th-Pb Geochronology". In: *Treatise on Geochemistry (Second*
 909 *Edition)*. Ed. by Heinrich D. Holland and Karl K. Turekian. Second Edition. Elsevier, pp. 341–
 910 378. DOI: [10.1016/B978-0-08-095975-7.00310-7](https://doi.org/10.1016/B978-0-08-095975-7.00310-7).
- 911 Scholle, Peter A and Arthur, Michael A (1980). "Carbon isotope fluctuations in Cretaceous
 912 pelagic limestones: potential stratigraphic and petroleum exploration tool". In: *AAPG Bul-*
 913 *letin* 64.1, pp. 67–87. DOI: [10.1306/2F91892D-16CE-11D7-8645000102C1865D](https://doi.org/10.1306/2F91892D-16CE-11D7-8645000102C1865D).
- 914 Schrag, Daniel P, Berner, Robert A, Hoffman, Paul F, and Halverson, G.P. (2002). "On the
 915 initiation of a snowball Earth". In: *Geochemistry, Geophysics, and Geosystems* 300. DOI:
 916 [10.1029/2001GC000219](https://doi.org/10.1029/2001GC000219).
- 917 Schrag, Daniel P, Higgins, John A, Macdonald, Francis A, and Johnston, David T (2013).
 918 "Authigenic carbonate and the history of the global carbon cycle". In: *science* 339.6119,
 919 pp. 540–543. DOI: [10.1126/science.1229578](https://doi.org/10.1126/science.1229578).
- 920 Skulan, Joseph, DePaolo, Donald J., and Owens, Thomas L. (1997). "Biological control of
 921 calcium isotopic abundances in the global calcium cycle". In: *Geochimica et Cosmochimica
 922 Acta* 61.12, pp. 2505–2510. DOI: [10.1016/S0016-7037\(97\)00047-1](https://doi.org/10.1016/S0016-7037(97)00047-1).
- 923 Staudigel, Philip T. and Swart, Peter K. (2019). "A diagenetic origin for isotopic variability of
 924 sediments deposited on the margin of Great Bahama Bank, insights from clumped isotopes".
 925 In: *Geochimica et Cosmochimica Acta* 258, pp. 97–119. DOI: [10.1016/j.gca.2019.05.002](https://doi.org/10.1016/j.gca.2019.05.002).
- 926 Swanson-Hysell, Nicholas L, Maloof, Adam C, Condon, Daniel J, Jenkin, Gawen RT, Alene, Mu-
 927 lugeta, Tremblay, Marissa M, Tesema, Tadele, Rooney, Alan D, and Haileab, Bereket (2015).
 928 "Stratigraphy and geochronology of the Tambien Group, Ethiopia: Evidence for globally syn-
 929 chronous carbon isotope change in the Neoproterozoic". In: *Geology* 43.4, pp. 323–326. DOI:
 930 [10.1130/G36347.1](https://doi.org/10.1130/G36347.1).
- 931 Swart, Peter K (2008). "Global synchronous changes in the carbon isotopic composition of
 932 carbonate sediments unrelated to changes in the global carbon cycle". In: *Proceedings of the
 933 National Academy of Sciences* 105.37, pp. 13741–13745. DOI: [10.1073/pnas.0802841105](https://doi.org/10.1073/pnas.0802841105).
- 934 Swart, Peter K and Eberli, Gregor P (2005). "The nature of the $\delta^{13}\text{C}$ of periplatform sediments:
 935 Implications for stratigraphy and the global carbon cycle". In: *Sedimentary Geology* 175.1-4,
 936 pp. 115–129. DOI: [10.1016/j.sedgeo.2004.12.029](https://doi.org/10.1016/j.sedgeo.2004.12.029).
- 937 Tang, Jianwu, Dietzel, Martin, Böhm, Florian, Köhler, Stephan J, and Eisenhauer, Anton
 938 (2008). " $\text{Sr}^{2+}/\text{Ca}^{2+}$ and $^{44}\text{Ca}/^{40}\text{Ca}$ fractionation during inorganic calcite formation: II. Ca
 939 isotopes". In: *Geochimica et Cosmochimica Acta* 72.15, pp. 3733–3745. DOI: [10.1016/j.gca.2008.05.033](https://doi.org/10.1016/j.gca.2008.05.033).
- 941 Tziperman, E., Halevy, I., Johnston, D. T., Knoll, A. H., and Schrag, D. P. (2011). "Biologically
 942 induced initiation of Neoproterozoic snowball-Earth events". In: *Proceedings of the National
 943 Academy of Sciences* 108.37, pp. 15091–15096. DOI: [10.1073/pnas.1016361108](https://doi.org/10.1073/pnas.1016361108).
- 944 Urey, Harold C (1947). "The thermodynamic properties of isotopic substances". In: *Journal of
 945 the Chemical Society (Resumed)*, pp. 562–581. DOI: [10.1039/JR9470000562](https://doi.org/10.1039/JR9470000562).
- 946 Urey, Harold C, Aten Jr., A.H.W., and Keston, Albert S (1936). "A concentration of the carbon
 947 isotope". In: *The Journal of Chemical Physics* 4.9, pp. 622–623. DOI: [10.1063/1.1749918](https://doi.org/10.1063/1.1749918).
- 948 Vahrenkamp, Volker C, Swart, Peter K, and Ruiz, Joaquin (1991). "Episodic dolomitization
 949 of late Cenozoic carbonates in the Bahamas; evidence from strontium isotopes". In: *Jour-*
 950 *nal of Sedimentary Research* 61.6, pp. 1002–1014. DOI: [10.1306/D4267825-2B26-11D7-8648000102C1865D](https://doi.org/10.1306/D4267825-2B26-11D7-8648000102C1865D).
- 952 Walker, James CG, Hays, PB, and Kasting, James F (1981). "A negative feedback mechanism
 953 for the long-term stabilization of Earth's surface temperature". In: *Journal of Geophysical
 954 Research: Oceans* 86.C10, pp. 9776–9782. DOI: doi.org/10.1029/JC086iC10p09776.
- 955 Wanninkhof, Rik (1985). "Kinetic fractionation of the carbon isotopes ^{13}C and ^{12}C during
 956 transfer of CO_2 from air to seawater". In: *Tellus B* 37B.3, pp. 128–135. DOI: [10.1111/j.1600-0889.1985.tb00061.x](https://doi.org/10.1111/j.1600-0889.1985.tb00061.x).

958 Westerhold, Thomas, Marwan, Norbert, Drury, Anna Joy, Liebrand, Diederik, Agnini, Claudia,
959 Anagnostou, Eleni, Barnet, James SK, Bohaty, Steven M, De Vleeschouwer, David, Florindo,
960 Fabio, et al. (2020). “An astronomically dated record of Earth’s climate and its predictability
961 over the last 66 million years”. In: *Science* 369.6509, pp. 1383–1387. doi: [10.1126/science.aba6853](https://doi.org/10.1126/science.aba6853).